Seasonal variations of metals and metalloids in atmospheric particulate matter (PM2.5) in the urban megacity Hanoi

Sandrine Chifflet, Léa Guyomarc'H, Pamela Dominutti, Lars-Eric Heimbürger-Boavida, Bernard Angeletti, Pascale Louvat, Jean-Luc Jaffrezo, Cam Tu Vu, Gaelle Uzu, Xavier Mari

Seasonal variations of metals and metalloids in atmospheric particulate matter (PM2.5) in the urban megacity Hanoi

Sandrine Chifflet[a*], Léa Guyomarc'h[a], Pamela Dominutti[b], Lars-Eric Heimbürger-Boavida[a], Bernard Angeletti[c], Pascale Louvat[d], Jean-Luc Jaffrezo[b], Cam Tu Vu[e], Gaelle Uzu[b], Xavier Mari[a,e,g]

[a] Aix Marseille University, Université de Toulon, CNRS, IRD, MIO (UM110), 13288 Marseille, France

[b] University of Grenoble Alpes, CNRS, IRD, INP-G, IGE (UMR 5001), 38000 Grenoble, France

[c] Aix Marseille University, CNRS, IRD, Collège de France, INRAE, CEREGE, 13545 Aix-en-Provence Cedex 4, France

[b] Université de Pau et des Pays de l'Adour, E2S UPPA, CNRS, IPREM, UMR 5254, Pau, France

[e] Water-Environment-Oceanography (WEO) Department, University of Science and Technology of Hanoi (USTH), Vietnam Academy of Science and Technology (VAST), 18 Hoang Quoc Viet, Hanoi, Vietnam

[g] IRD, Chulalongkorn University, 254 Henri Dunant Road, Pathumwan, 10330 Bangkok.

[*] Corresponding author: sandrine.chifflet@mio.osupytheas.fr; Phone: + 33 4 86 09 05 32;

For submission to Atmospheric Pollution Research

September 2023 (revised version)

Abstract

Fine particulate matter (PM2.5) in the atmosphere is of particular concern due to its adverse effects on human health and its impact on global warming. southeast Asia is a hot spot for fossil fuel combustion with recurrent release of large plumes spreading over the ocean and neighbouring countries. Due to the complex mixture of PM2.5, the atmospheric sources contribution related to local and regional emissions in Hanoi (northern Vietnam) is still ill-constrained. Here, we present a year-round study (November 2019 to December 2020) with measurements of 18 metals and metalloids (MM) and lead isotopes in the PM2.5 fraction to quantify weather-related atmospheric inputs and to assess risk to human health. Anthropogenic inputs from fossil fuel combustion accounted for about 80% in PM2.5. We found high PM2.5-bound MM concentrations often exceeding national and global standards with a low risk of chronic inhalation and carcinogenicity, mainly attributable to Cr. During winter monsoon (northeastern winds), stable weather conditions led to the enrichment of long-range air mass transport of local particulate emissions. During the summer monsoon (southeastern winds), warm and moist winds reduced coal contribution in PM2.5. Our study highlights the need for a strict implementation of policies to control hazardous MM emissions by reducing fossil fuel combustion. On the one hand, reducing coal-related activities could reduce Cr emissions and therefore improve the risks to human health. On the other hand, public policies should encourage conversion to green transport in order to reduce petrol combustion and thus limit global warming.

Keywords: contamination, mercury, lead isotopes, atmospheric transport, fossil fuel combustion

1. Introduction

Atmospheric particulate matter (PM) alters the climate (Fuzzi et al., 2015) and has a negative effect on human health (Janssen et al., 2011; Pope et al., 2011; Xing et al., 2016). Fine particles smaller than 2.5 µm (PM2.5) can penetrate deep into the lungs and cause asthma, lung disease, heart disease and cancer, depending on the amount inhaled and the time of exposure and the susceptibility of the person. Globally, inhalation of atmospheric PM is currently estimated to cause 3.3 million premature deaths per year worldwide, and could double by 2050 (Stanaway et al., 2018; Lelieveld et al., 2020). Atmospheric PM is a complex mixture of various compounds such as organic and elemental carbon, sugars, polycyclic aromatic hydrocarbons, secondary inorganic aerosol (*e.g.,* SO_4^{2-}, NH_4^+, NO_3^-), *etc.* (Finlayson-Pitts et al., 2020).

Among these compounds, metals and metalloids (MM) are of particular concern for human health (Palleschi et al., 2018; Rafiee et al., 2020; Soetrisno and Delgado-Saborit, 2020). In small amounts, MM are essential to maintain biological functions, but in larger amounts they can damage cellular functions and cause toxicity in certain organs such as kidneys, brain, blood, skin, heart (Mitra et al., 2022). Due to their chemical coordination and oxidation-reduction properties, at high concentrations, MM can compete with each other. One element can bind to protein sites in place of another, causing DNA damage and perturbing protein function and enzyme activity (Balali-Mood et al., 2021; Witkowka et al., 2021; Jaishankar et al., 2014). Among them, As, Cd, Cr are of greatest concern due to their numerous sources of emissions, high toxicity, and persistence in urban areas (Li et al., 2021).

Atmospheric PM is ubiquitous and can originate from natural and anthropogenic sources (Pacyna and Pacyna, 2001; Gieré and Querol, 2010). PM-bound MM can be naturally introduced into the atmosphere through wind erosion of soil or sea surface, volcanic emissions and forest fires, mainly as coarse fraction (> 3-4 µm) and relatively non-solvable (Li et al., 2009; Bacon et al., 2011). By contrast, MM from anthropogenic activities can be introduced into the atmosphere through many pathways such as fossil fuel combustion, mining, ferrous and non-ferrous metal manufacturing, industrial production (*e.g.,* cement, ceramic, glass, fertilizers), road traffic, waste incineration,

74 domestic heating *etc.* (Pacyna et al., 2007; Hao et al., 2018). Furthermore, anthropogenic MM tend
75 to be associated with fine particles (Hein et al., 2022) and far exceed natural concentrations in
76 heavily urbanized/industrialized areas (McNeill et al., 2020; Guo et al., 2023).

77 Atmospheric PM is a global concern and even more so for densely populated Asian countries
78 (Xu et al., 2020; Zhang et al., 2021; Sakunkoo et al., 2022). Vietnam's capital of Hanoi experienced
79 rapid urbanization over the last decades, resulting in a severe increase in PM2.5 atmospheric load
80 with an average annual concentration greater than 45 µg m^{-3} (Makkoken et al., 2023), well above
81 national (25 µg m^{-3}, QCVN 05:2013/BTNMT) and updated global guidelines (5 µg m^{-3}; WHO, 2021).
82 During peak hours, congested traffic significantly increases fine particulate emissions, contributing up
83 to 40% of PM2.5 (Cohen et al., 2010; Quang et al., 2021). Northern Vietnam is heavily industrialized
84 with coal-fired power plants as the main source of energy (Huy and Kim Oanh, 2017; Roy et al.,
85 2021). Furthermore, agricultural burning is widely used in rural and suburban areas (Lasko et al.,
86 2018; Le et al., 2020). In addition, long-range air mass transport from China to northern Vietnam
87 contribute to the increase in PM2.5, with concentrations regularly exceeding 150 µg m^{-3} during the
88 northeast winter monsoon (Ly et al., 2021; Ngoc et al., 2021; Makkoken et al., 2023).

89 Although PM2.5-bound MM are strongly studied in China (*e.g.,* Liao et al., 2023; Zhou et al.,
90 2023; Guo et al., 2022; Duan et al., 2021), the latter are poorly documented in Vietnam. In 2020,
91 mean annual concentrations for As, Cd, Cr in PM2.5 were found at 6.2, 1.9, 9.4 ng m^{-3}, respectively
92 (Nguyen et al., 2022), exceeding global guidelines for As and Cr (6.0 and 0.25 ng m^{-3}, respectively;
93 WHO, 2021). In addition, a strong variability in PM2.5-bound MM can be observed between studies.
94 In Hanoi, over the same sampling periods (2001 - 2008 and 2002 - 2005), the mean Pb concentration
95 in PM2.5 was assessed to 236 ng m^{-3} (Cohen et al., 2010) and 137 ng m^{-3} (Hopke et al., 2008),
96 respectively, namely a difference greater than 50% between the two studies. In addition, maximum
97 measured values were three times lower in 2001 - 2008 than in 2002 - 2005 (5.4 and 15.0 µg m^{-3},
98 respectively), but these results are well above the WHO guidelines (0.15 µg m^{-3}; WHO, 2021) for the
99 two studies.

Principal Component Analysis (PCA) is a statistical technique widely used to identify the sources of MM, but the correlation matrices are poorly weighted and do not allow them to be quantified. Alternative techniques using Chemical Mass Balance (CMB) or Positive Matrix Factorization (PMF) are mathematical techniques used to solve systems of linear equations. The CMB model requires a large number of samples and the identification of sources is based on the chemical profiles from data obtained mainly in northern America, which may be different for southeast Asia (Henry et al., 1984, Paatero and Tapper, 1994; Pant and Harrison, 2012). With the PMF model, results are constrained to provide positive source contributions, and the uncertainty weighted difference between the observed and predicted species concentration is minimized. However, analyses of large datasets are often time-consuming and use up all the computer's available memory, which slow down the programme and can even cause errors (Hopke, 2000). Using PMF model, Cohen et al. (2010) found that the main sources of PM2.5 in Hanoi were from traffic (40 ± 10%), industry (19 ± 8%), and coal (17 ± 7%). The contribution of sources related to local and regional PM2.5 emissions is still under debate (Nguyen et al., 2020). In a recent study, Makkonen et al. (2023), found that PM2.5 in Hanoi are from local and regional secondary inorganic emissions (18 and 25%, respectively), biomass burning (19%), dust (17%), traffic (12%) and industry (9%). Given the high concentrations of PM2.5 and associated MM already observed, it is important to better define and assess anthropogenic contributions in order to limit the risk of exposure to human health. (Nguyen et al., 2022; Vo et al., 2022).

Isotopic analyses are commonly used for the identification and quantification of MM sources (Chifflet et al., 2018). Although the stable radiogenic lead isotopic composition (^{206}Pb, ^{207}Pb and ^{208}Pb) can be naturally transferred in the environment *via* weathering processes (Stacey and Kramers, 1975), these isotopes are not significantly affected by physico-chemical fractionation processes after mixing with secondary Pb sources thus providing an efficient tool for determining the origins and pathways of Pb pollution (Komárek et al., 2008). In order to better assess the impact of anthropogenic activities on air quality, we are presenting here a year-round study (November 2019

to December 2020) with quantitative measurements of 18 MM (Ag, Al, As, Cd, Co, Cr, Cu, Fe, Hg, Mn, Ni, Pb, Sb, Sn, Ti, U, V and Zn) and lead isotopes analyses (^{206}Pb, ^{207}Pb and ^{208}Pb) in PM2.5 collected in Hanoi. The objectives are i) to identify and quantify the main anthropogenic sources, ii) to study the impact of weather conditions on MM variability in PM2.5 and, iii) to assess potential inhalation risks to human health per MM. Given the energy demand in Southeast Asia and the population density of Hanoi, the objective of this article is not to conduct an exhaustive study of PM2.5 sources but to focus on the impact of fossil fuels combustion on air quality.

2. Materials and Methods

2.1 Study site

Hanoi is a megacity covering an area of 3,359 km² with a population of 5.2 million in 2023 (Makkoken et al., 2023). The city is located in the Red River delta (northern Vietnam) about 100 km from the Gulf of Tonkin (Fig. 1). The subtropical climate is mainly influenced by the northeast monsoon in winter (November to March) and the southeast monsoon in summer (May to September) with two short intermediate seasons in spring and fall (Ngu and Hieu, 2004). In winter, the high atmospheric pressure above central China brings cold and calm air masses to northern Vietnam, the low boundary mixing layer favouring the accumulation of local atmospheric particles (Hai and Kim Oanh, 2013). In summer, the high atmospheric pressure moves toward the southern hemisphere bringing wet and warm air masses to Hanoi (Hien et al., 2002).

Hanoi is surrounded by many suburban industrial activities (*e.g.,* Thang Long industrial Park in the North, Saidong industrial zone in the East, Ngoc Hoi industrial zone in the South) and several highly industrialized provinces in northern Vietnam (Thai Nguyen, Quang Ninh, Bac Ninh, and Hung Yen) (Hien et al., 2020). Approximately 10 coal-fired power plants are located within 200 km of Hanoi and emit large amounts of PM into the atmosphere (https://globalenergymonitor.org/projects/global-coal-plant-tracker/tracker/). In addition, the

vehicle traffic increases sharply together with the expansion of urban and industrial activities. In 2019, more than 6.6 million vehicles were registered in Hanoi (0.7 million cars and 5.8 million motorcycles) causing serious congestion problems on some roads during peak hours (Huu and Ngoc, 2021).

2.2 Sampling

PM2.5 were collected on the roof top of the University of Science and Technology of Hanoi (USTH; 21.0489°N, 105.8011°E) using a Staplex High Volume Air sampler. The sampling was conducted from November 2019 to December 2020 (14 months) with quartz fiber filters (Staplex Type TFAQ810 of 20x25 cm). PM2.5 samples (n = 27) were collected weekly over 24-hour periods (1 sample per week), except during the lockdown in April 2020 due to COVID-19 pandemic (corresponding to 4 "missing" samples as of 31/03/2020, 07/04/2020, 14/04/2020 and 21/04/2020). The average air volume filtered –calculated using the recorded air flow and the sampling time– was 1803 ± 81 m^3 $filter^{-1}$. Filters were pre-combusted (550°C, 12h) before sampling to prevent organic matter and mercury residue (US EPA 2013). Field blanks were handled identically to the PM2.5 sampling, but were run on the Staplex sampler for only 1 min (Pekney and Davidson, 2005). The quartz filters were kept frozen in clean aluminium foils and plastic bags until laboratory analyses.

2.3 Weather conditions

During the study, weather data (wind speed and direction) were downloaded from the National Oceanic and Atmospheric Administration (NOAA, USA) station at Noibai International Airport (21.2212°N, 105.8072°E), 12 m above ground level. The NOAA station was located 23 km North of the USTH. Local precipitation was downloaded online (https://www.historique-meteo.net/asie-sud-est/vietnam/2020/05/).

For each sampling period, the NOAA's Hybrid Single-Particle Lagrangian Integrated Trajectory model (NOAA HYSPLIT; Stein et al., 2015; Rolph et al., 2017) was used to draw 24 h backward air

mass trajectories based on weather data in the Global Data Assimilation System (GDAS) archive starting at 8 am (01:00 UTC) with a temporal resolution of 1 hour at the sampling site and the height of 500 m (Fig. S1). However, the accuracy of an individual trajectory is limited by various uncertainties, leading to coarse approximation of air mass origin (Draxler et al., 2022). Large numbers of trajectories were statistically used to identify homogeneous groups of transport pathways. Weather conditions (wind roses and trajectory frequencies) grouped by seasonal variations (winter and summer monsoon, intermediate spring and fall) are presented in Fig. 2 using the HYSPLIT model available online (https://www.ready.noaa.gov/HYSPLIT.php).

2.4 Laboratory analyses

2.4.1 Metals and metalloids (MM)

Sample processing was carried out in a clean laboratory (ISO 5) at the MIO (Aix Marseille University), using bi-distilled (HCl and HNO_3) and commercial grade (HF; Optima grade, Fisher Chemical) acids as well as ultrapure water (Milli-Q Integral 3, Millipore). The perfluoroalkoxy vials (PFA vials, Savillex) were pre-cleaned in two acid baths (HCl 10%, 90°C, 24 h and HNO_3 10%, 90°C, 24 h). The analytical tubes (metal-free centrifuge tubes, VWR) were pre-cleaned in HCl (10%) overnight at room temperature. PFA vials and analytical tubes were thoroughly rinsed then dried under a laminar flow hood (ISO 1) before using. Sub-samples (47 mm punch diameter) were digested in PFA vials in a mixture of pure acids (HNO_3, 2 mL; HCl, 2 mL; HF, 1 mL), heated at 120°C during 24 h, evaporated to near dryness, and re-dissolved into 3 mL of HNO_3 (2% v/v). The digested samples were then diluted in analytical tubes using HNO_3 (2% v/v) before running MM analyses (modified method 3050B; US EPA, 1996).

MM (Ag, Al, As, Cd, Co, Cr, Cu, Fe, Mn, Ni, Pb, Sb, Sn, Ti, U, V and Zn) analyses were performed using an inductively-coupled plasma mass spectrometer (ICP-MS NexION 300; Perkin Elmer) at the LA-ICP-MS platform (CEREGE, Aix Marseille University). Indium was used as internal standard to correct for instrumental mass bias. The digestion procedure was assessed using two

certified samples, from marine sediments (MESS4, National Research Council of Canada), and from atmospheric PM (NIST1649b, National Institute of Standard and Technology, USA). Our determinations of MM concentrations in certified samples were within the satisfactory target recovery of 100 ± 15% (Chen and Ma, 2001). All MM concentrations in PM2.5 were blank corrected. The latter had values below 1% for most MM, except for Al, Cr, Ni and U, which had values of approximatively 3%. Quality control details are presented in Table S1.

2.4.2 Mercury

For total Hg determination, sub-samples (47 mm punch diameter) were analysed by atomic absorption spectrometry after thermal calcination (AMA-254, Leco). The method detection limit, estimated as three times the standard deviation of blank samples, was 20 pg. The certified reference material (MESS4, National Research Council of Canada) was run several times per analytical batch and systematically before starting the measurements to check the accuracy of the measurements. The measured values were always within ± 5% of the recommended values.

2.4.3 Lead isotopes

Lead isotopic analyses (^{206}Pb, ^{207}Pb, ^{208}Pb) were performed using a multi collector inductively coupled plasma mass spectrometer (MC-ICP-MS; Nu Instrument) at the I3 platform (IPREM, University of Pau and Pays de l'Adour). All sample preparations were carried out in clean laboratories (MIO, Aix Marseille University). Acids used were either bi-distilled (HCl and HNO_3) or commercial (HBr; Optima, Fisher Chemical). In order to minimise matrix effects during analysis, Pb was extracted from digested samples (see section 2.4.1) and purified by an ion exchange resin (Dowex 1X8, 100-200 mesh, Acros Organics) according to a conventional protocol (Monna et al., 1997; Ortega et al., 2012). The purified Pb samples were introduced into the MC-ICP-MS as dry aerosol (*via* an APEX nebulizer attached to a SPIRO membrane; ESI) at 50 µg L^{-1}. An internal Tl isotopic standard (NIST997; National Institute of Standard and Technology, USA) was added at 12.5 µg L^{-1} to all samples to correct mass

fractionation effects. In addition, a standard bracketing method was applied to correct the instrumental drift with a Pb isotopic standard (NIST981; National Institute of Standard and Technology, USA). Blank and Pb standard (NIST981) were run several times per analytical batch for the quality control procedure. The averages of the measured $^{207}Pb/^{206}Pb$ and $^{208}Pb/^{206}Pb$ ratios (n = 70) in these standards were 0.9144 ± 0.0002 and 2.1662 ± 0.0011, respectively, matching with the respective reference values of 0.9146 ± 0.0003 and 2.1681 ± 0.0008.

2.5 Data processing

2.5.1 Reconstructed mass

PM2.5 was estimated using mass reconstruction equations (Querol et al., 2001; Putaud et al., 2010; Chow et al., 2015). Briefly, the concentration of PM2.5 is expressed as the sum of its representative chemical components, including: inorganic major ions (NH_4^+, NO_3^-, SO_4^{2-}); organic carbon (OC); elementary carbon (EC, also known as black carbon or BC); geological minerals (Al, Ca, Fe, K, Mg, Mn, Ti, P); sea salts (Na^+) and other elements (Cu, Ni, Pb, V, Zn). Chemical analyses were performed at the Air-O-Sol analytical platform (IGE, Grenoble Alpes University). Details of the PM2.5 mass reconstruction are presented in supplementary information.

2.5.2 Sources apportionment of Pb

In Vietnam, Pb could come mainly from natural (soil) and anthropogenic (fossil fuel combustion) sources. Therefore, the contribution of each source could be assessed using Pb isotopic ratios ($^{207}Pb/^{206}Pb$ and $^{208}Pb/^{206}Pb$) with the following linear mixing model (Monna et al., 1997; Chifflet et al., 2018):

$$\left(\frac{^{207}Pb}{^{206}Pb}\right)_{PM2.5} = x_1\left(\frac{^{207}Pb}{^{206}Pb}\right)_1 + x_2\left(\frac{^{207}Pb}{^{206}Pb}\right)_2 + x_3\left(\frac{^{207}Pb}{^{206}Pb}\right)_3 \quad (1)$$

$$\left(\frac{^{208}Pb}{^{206}Pb}\right)_{PM2.5} = x_1\left(\frac{^{208}Pb}{^{206}Pb}\right)_1 + x_2\left(\frac{^{208}Pb}{^{206}Pb}\right)_2 + x_3\left(\frac{^{208}Pb}{^{206}Pb}\right)_3 \quad (2)$$

$$x_1 + x_2 + x_3 = 1 \quad (3)$$

where the numbers in subscript (1, 2 and 3) represent sources, and *x* their relative contribution.

2.5.3 Health risk assessment

Health risk assessment provides indexes of adverse health effects for a specific group of population over a specific period (US EPA, 2005). It can be expressed as hazard quotient to assess the non-carcinogenic risk (HQ) and carcinogenic risk (CR). Some MM involved in carcinogenic processes were classified by the International Agency for Research on Cancer (IARC, 2023) as hazardous carcinogens (Group 1: As, Cd, and Cr^{IV}), probably carcinogens (Group 2A: Pb and $Co^{0,II}$), carcinogens (Group 2B: Ni, Ti, and V), pollutants of potential interest (Group 3: Hg^{0}, Mn, Co^{III}, and $Cr^{0,III}$).

The inhalation exposure concentration (EC, μg m^{-3}) was expressed as follows (US EPA, 2009):

$$EC_i = \frac{C_i^{95\%} \times ET \times EF \times ED}{AT_n} \quad (4)$$

where $C_i^{95\%}$ is the mean concentration (95% upper confidence limit) of a metal or metalloid in PM2.5 (μg m^{-3}); *ET* is the exposure time (24 h d^{-1}); *EF* is the exposure frequency (365 d yr^{-1}); *ED* is the exposure duration (yr); and AT_n is the averaging time (= *ED x 365 d x 24 h* d^{-1} and *70 yr x 365 d* yr^{-1} *x 24 h* for non-carcinogens and carcinogens, respectively). The reference values (*ET, EF, ED* and AT_n) are from the EPA Integrated Risk Assessment System (EPA IRIS) website (https://epa.gov/iris).

The mean concentration of a metal or metalloid in sample ($C_i^{95\%}$) is considered as the reasonable maximum exposure and was calculated as follows (Zhang et al., 2021):

$$C_i^{95\%} = exp\left(\overline{lnC_i} + 0.5 \times S_{lnCi}^2 + \frac{S_{lnCi} \times H_{0.95}}{\sqrt{n-1}}\right) \quad (5)$$

where $\overline{lnC_i}$ and S_{lnCi} are the arithmetic mean and standard deviation of the log-transformed C_i, respectively; *n* is the number of samples. Statistical $H_{0.95}$ values that depend on S_{lnCi}, *n*, and the confidence level (0.05) are taken from Gilbert (1987).

The non-carcinogenic (HQ) and carcinogenic (CR) risks associated with chemical inhalation exposure were calculated as follows (US EPA, 2009):

$$HQ_i^{inh} = \frac{EC_i}{RfC_i \times 1000} \quad (6)$$

$$CR_i^{inh} = EC_i \times IUR_i \quad (7)$$

where RfC_i and IUR_i are the reference concentration and the inhalation unit risk for a metal or metalloid *i*, respectively. $HQ_i > 1$ indicates a potential chronic effect through inhalation of a metal or metalloid *i*. CR_i indicates the probability that a person will develop cancer by inhaling certain MM with varying risk of very low ($CR \leq 10^{-6}$), low ($10^{-6} \leq CR < 10^{-4}$), moderate ($10^{-4} \leq CR < 10^{-3}$), high ($10^{-3} \leq CR < 10^{-1}$), very high ($CR \geq 10^{-1}$) (Hu et al., 2012; Roy et al., 2019; Behrooz et al., 2021). To assess the risk of exposure to multiple MM, the cumulative HI and TCR indexes were calculated as the sum of individual HQ_i and CR_i, respectively. Updated reference values (RfC_i and IUR_i) can be found on the Office of Environmental Health Hazard Assessment website (https://dtsc.ca.gov; OEHHA, 2019) or in Zhang et al. (2021) and shown in Table S2.

2.6 Multivariate statistical analyses

Statistical analyses were performed using Xlstat software package version 2022.2.1 (Addinsoft 2023, Boston, USA, https://www.xlstat.com). First, the normality and homoscedasticity of data were tested. Then, Principal Component Analysis (PCA) and Hierarchical Cluster Analyses (HCA) were applied to explain the temporal variability of MM in PM2.5. The Pearson correlation matrix was used to examine the relationships between concentrations of the various MM. The Ward's method with Euclidean distances was used to assess similarity or dissimilarity between samples. All statistical tests were performed with a probability (p) < 0.05.

3. Results

3.1 Temporal variations of PM2.5 and MM concentrations

PM2.5 concentrations varied from 8.3 to 148 µg m^{-3} during the sampling period (November 2019 to December 2020) (Fig. 3; Table S3). High concentrations were observed mainly during the winter monsoon, dominated by east and northeast winds. Conversely, low PM2.5 concentrations

were observed during the summer monsoon, dominated by southeast or southwest winds. This monitoring was consistent with recent studies of PM2.5 levels in Hanoi (Ngoc et al., 2021, Ly et al., 2021; Bui et al., 2022; Voung et al., 2023). The average annual concentration (40.2 ± 26.3 µg m^{-3}) was 1.6 and 8.0 times higher than the national standard (25 µg m^{-3}; QCVN 05:2013/BTNMT) and the World Health Organization guidelines (5 µg m^{-3}; WHO, 2021), respectively. For the 24-hour exposure to PM2.5, 31.6% and 89.5% of the samples had concentrations above the national standard (50 µg m^{-3}; QCVN 05:2013/BTNMT) and the WHO guidelines (15 µg m^{-3}; WHO, 2021), respectively. Although very low precipitation (near 0 mm d^{-1}) was recorded in winter and spring, a large increase in precipitation was observed from summer onwards, reaching a maximum of 135 mm d^{-1} in October 2020. Wind speed was variable (2.81 ± 0.85 m s^{-1}) during the sampling period but the lowest values were recorded in winter.

Statistical data (average, minimum and maximum) for PM2.5-bound MM concentrations over the sampling period are presented in Table 1 and detailed values per sample in Table S4. PM2.5-bound MM average concentrations varied over several orders of magnitude, with Al, Fe and Zn being the most abundant (higher than 300 ng m^{-3}), followed by Cu, Mn, Pb and Ti (between 30 and 60 ng m^{-3}), As, Cd, Cr, Ni Sb, Sn and V (between 1 and 5 ng m^{-3}), and other MM (Ag, Co, Hg and U) at less than 0.3 ng m^{-3}. These results are in good agreement with previous studies in Hanoi (Nguyen et al., 2022; Bui et al., 2022; Vuong et al., 2023). No information was found to compare these values with the recommendations of national or global health organizations. However, for PM10 (atmospheric particulate matter < 10µm in aerodynamic diameter), the European Community and the WHO recommend limiting annual exposure to Pb, Ni, As, Cd and Cr^{VI} to 150, 20, 6, 5, and 0.25 ng m^{-3}, respectively (Directives 2008/50/EC; 2004/107/EC; WHO, 2021). In the present study, some targeted MM (Pb, As, Cd and Cr) had 24-hour maximum concentrations above the annual exposure guidelines.

3.2 Principal Component Analysis and clustering

The Pearson correlation matrix and Ward's Euclidean distances were examined to highlight the links between PM2.5-bound MM and weather data (wind speed, precipitation and wind direction as qualitative values). High and significant correlations ($r > 0.6$ and $p < 0.05$, $n = 57$) were observed between all variables except Ag, Cu and Precipitation (Table S5). Although wet deposition is considered a major process for removing particulate-bound MM, transfer mechanisms depend on particle size and metal solubility (Pan and Wang 2014; Jaffrezo and Colin, 1988). PM10 is more readily recovered than PM2.5 (Cheng et al., 2021; Zhou et al., 2021) and only the soluble fraction of MM is cleaned from particles (Vithanage et al., 2022). These considerations may explain the lack of correlation between PM2.5-bound MM and precipitation. In addition, the 24-hour sampling conducted on 10/12/2019 and 12/05/2020 made high contribution (26 and 40%, respectively) to factors loadings focusing multivariate statistical analyses on these two specific events instead of the overall study. These two events were characterized by maximum concentrations of PM2.5, Al, Ti, Fe, Co, Pb and Hg on 10/12/2019 and, a low concentration of PM2.5 associated with high concentrations of Ni and Cr on 12/05/2020.

To better assess the impact of seasonal variations PM2.5-bound MM, multivariate statistical analyses were reviewed without these two samples, and by redefining some variables (wind speed and direction, precipitation, Ag and Cu) as illustrative parameters (Fig. 4). The original variables were reduced to two factors (F1 and F2) explaining 65% of the total variance with eigenvalues > 1. F1 had a high positive loading for all MM and negative loading for weather data (wind speed and precipitation). F2 had a high positive loading for Al, Cr, Co, Fe, Ni, Ti, U, and V and a negative loading for As, Cd, Hg, Mn, Pb, Sb, Sn and Zn. The scatter plot corresponding to samples showed two clusters (C1 and C2) clearly distributed along F1 axis with a positive barycentre for C2 and a negative barycentre for C1. Although PM2.5 in C1 could have originated from different air mass trajectories, PM2.5 in C2 all originated from northerly or north-easterly winds (Table S6).

3.3 Lead isotopes

The complex mixture of particles does not allow for accurate quantification of anthropogenic sources using statistical studies alone. Due to quantum theory, isotopes are powerful tools for tracing Pb sources and atmospheric transport pathways. Although the isotopic composition of stable radiogenic lead (^{206}Pb, ^{207}Pb and ^{208}Pb) is naturally transferred in the environment (Bollhöfer and Rosman 2000), this composition may vary after mixing with secondary sources emitted by anthropogenic activities (Zheng et al., 2004; Komárek et al., 2008). Despite the phase-out of leaded gasoline in southeast Asia over the past two decades, anthropogenic Pb inputs are still large enough to accurately quantify its sources of emissions (Mukai et al., 2001a; Bing-Quan et al., 2001; Yao et al., 2015). Lead isotopic ratios in PM2.5 collected during the sampling period ranged from 0.8005 to 0.8702 for ^{207}Pb/^{206}Pb and from 1.9754 to 2.1149 for ^{208}Pb/^{206}Pb (Table S7). These ratios were consistent with those found locally in the Tay Ho urban lake in Hanoi (Kikuchi et al., 2010) or with PM10 collected in Haiphong (Chifflet et al., 2018) showing the good relevance of the results.

4. Discussion

4.1 Sources identification

Atmospheric particle are highly dynamic and reactive compounds whose chemical composition is attributed to a wide range of natural and anthropogenic sources (Laskin et al., 2019). Because PM-bound MM depend primarily on soil composition, raw material use, and primary energy sources (from oil and coal combustion), elemental ratios are widely used to identify emission sources (*e.g.*, Okuda et al., 2004; Hopke and Cohen, 2011). For example, V/Ni is well-known as indicator oil combustion (Pacyna and Pacyna, 2001). Previous studies have reported typical V/Ni ratios in heavy oil combustion for ship engines (with values between 3 – 4, Mazzei et al., 2008), in oil combustion for household heating (2.4; Lee et al., 2000) or in road traffic (1.49; Thorpe and Harrison, 2008). In addition, low V/Ni ratios (0.5) have also been reported in Chinese megacities (Beijing, Changchun and Chengdu) and attributed to PM from traffic and/or coal mining activities (Xu et al., 2020). Finally,

V/Ni ratios of 0.55 and 0.15 have also been found in Vietnamese coal and diesel, respectively (Chifflet et al., 2018). In this study, the V/Ni ratios in PM2.5 ranged from 0.7 to 2.8, showing the mixing of various sources (probably from fossil fuel combustion). A specific trend (V/Ni = 0.15, r^2 = 0.98, n = 3) was also observed in the spring under easterly winds with V/Ni highlighting the impact of road traffic in the samples (Fig. 5a).

Coal combustion, industrial smelting and waste incineration are important sources of Cd and Pb in atmospheric particles (Pacyna and Pacyna, 2001; Sun et al., 2010; Tang et al., 2013; Sun et al., 2014). Generally, Cd/Pb ratios in urban/industrial cities in Asia have values close to 0.033 in Taiwan (Chen et al., 2015), 0.030 in Taipei (Hsu et al., 2005), 0.025 in Beijing and Changchun and 0.049 in Chengdu (Xu et al., 2020). In Europe, same ratios (0.029) have also been observed in the steel industry (Oravisjarvi et al., 2003) and higher values (0.08) have been found in municipal waste incinerators (Font et al., 2015). Conversely, lower Cd/Pb ratios have been found in natural Asian soils (0.017; Hsu et al., 2005) or rural European villages (0.013; Font et al., 2015). In this study, the Cd/Pb ratios in PM2.5 showed two trends with values close to 0.032 (r^2 = 0.96; n = 48) or close to 0.012 (r^2 = 0.99; n = 8) (Fig. 5b). Although the highest trend appears to be independent of weather conditions, the lowest trend was observed with southeasterly winds and rainy days. These results could indicate a dominant emission of PM2.5 from local urban/industrial activities throughout the year and a predominance of natural inputs of PM2.5 in specific weather conditions. In addition, high Cd/Pb ratio (0.088) was also observed during a specific event (18/02/2020) probably related to waste incineration emissions.

Sb is mainly derived from anthropogenic sources, in particular emissions from brake pad wear (Varrica et al., 2013) as well as, more broadly, from industrial activities and fossil fuel combustion (Pacyna and Pacyna, 2001; Tian et al., 2014). A specific Sb/Cd ratio of 5.0 has been attributed to road brake pad wear (Thorpe and Harrison, 2008) A lower Sb/Cd ratio can also be found

409 in Chinese and Vietnamese coal but the value varies by geographical area. Indeed, a Sb/Cd ratio of
410 1.2 was found in the Liupanshui coal mine (Guizhou, southwest China; Zhuang et al., 2000) and an
411 average of 0.9 (n = 1,123) was proposed for the whole country (Dai et al., 2012). However, coal mines
412 in northern Vietnam are rich in organic sulphur and enriched with Sb thus increasing the Sb/Cd ratio
413 (Li et al., 2023). For example, a Sb/Cd ratio of 3.0 was found in the Coc Sau coal mine (Chifflet et al.,
414 2018). In this study, high variability in Sb/Cd ratios was observed in PM2.5, indicating a possible mix
415 of different anthropogenic sources (Fig. 5c). Three trends were observed during the sampling period
416 with Sb/Cd ratios close to 4.3 ($r^2 = 0.99$; n = 32), close to 2.6 ($r^2 = 0.99$; n = 14) or close to 1.3
417 ($r^2 = 0.92$; n = 11). Although the weakest trends are observed by east and northeast winds
418 (Sb/Cd = 1.3) or northeast and southeast winds (Sb/Cd = 2.6), the highest trend (Sb/Cd = 4.3) does
419 not appear to be influenced by wind direction. These results seem to confirm the predominance of
420 regional and local PM2.5 emissions from coal activities mixed with local PM2.5 emissions from road
421 traffic..

422 Rapid urbanisation and industrialisation in southeast Asia, as well as long-range
423 transboundary transport of atmospheric PM, make it difficult to assess the presence of natural
424 sources in this region. In general, natural particles are emitted by wind erosion of soils in arid regions.
425 MM concentrations from pristine soil in Vietnam are missing. However, soil dust appears to be the
426 dominant source of Al and Ti in Hanoi (Hein et al., 2022) and a significant Al/Ti ratio of 14.5 (r^2 =0.98;
427 n = 54) is observed in this study (Fig. 5d). Same Al/Ti ratio (14.3) was also found in PM2.5 collected
428 during sand dust storms in northern Chinese megacities (Xu et al., 2004a; Shen et al., 2007) showing
429 a possible long-range transport of atmospheric PM. In Seoul (North Korea), the variation in the Al/Ti
430 ratio was closely related to atmospheric transport of particles from the Gobi Desert through China
431 and Mongolia (Al/Ti = 23.5) or particles emitted locally by soil resuspension (Al/Ti = 15.2) (Kim et al.,
432 2003). In addition, an average Al/Ti of 25 was proposed for the upper continental crust (Wedepohl,
433 1995). These results show the likely mix between natural dust and urban dust in this study.
434

435 *4.2 Effect of local and regional air mass transport on source distribution*

436 4.2.1 Impact of weather conditions on MM concentrations

437 PM typically persists in the atmosphere between a few days and several weeks before being
438 scavenged by dry or wet deposition (Seinfeld 2014). During their lifetime, they may travel long
439 distances between the source of emission and the deposit area, undergoing chemical and physical
440 transformations. Therefore, weather conditions can strongly influence their concentrations and the
441 MM. In this study, the PCA-HCA analyses showed that high MM concentrations in cluster C2 occurred
442 with north or northeast winds during the winter monsoon (Fig. 4). In addition, in C2, PM2.5
443 concentrations increased as the wind speed decreased (Fig. S2). Such results have already been
444 observed in Hanoi (Hai and Kim Oanh, 2013; Nguyen et al., 2022; Makkoken et al., 2023). This pattern
445 is attributed to recurring temperature inversion events in air layers in winter monsoon, thus limiting
446 the dispersion of PM (Hien et al., 2002; Ly et al. 2021).

447 In winter, a ridge of high-pressure flows air masses from Siberia to China towards northern
448 Vietnam, bringing cold and dry air, enriched by anthropogenic particles during their long-range
449 transport. However, this is not the only pathway that controls the transport of particles in Hanoi. The
450 height of the boundary layer at the Earth's surface also plays an important role in vertical mixing.
451 Previous studies have shown that high concentrations of elemental carbon (*i.e.,* black carbon
452 produced by incomplete combustion of fossil fuels) reduces vertical mixing (Wilcox et al., 2016; Hu et
453 al., 2020; Duc et al., 2023). This is because the black carbon emitted in the upper air mass absorbs
454 the sunlight, which heats up faster than the air mass closest to the Earth's surface (Ding et al., 2016).
455 As a result, black carbon induces a reduction in turbulent kinetic energy in the surface mixed layer,
456 which promotes its enrichment by local particle emissions (Petäjä et al., 2016). Conversely, during
457 the summer monsoon, winds from the southeastern South China Sea and the sub-tropical western
458 Pacific carry warm, moist, particle-depleted air. High temperatures enhance strong atmospheric
459 convection, thus improving the dispersion of anthropogenic emissions (Hein et al., 2002; Yang et al.

2018). In addition, heavy precipitation during the intermediate fall periods further decreases PM2.5 (and bound MM) due to the scavenging effects (Wang et al. 2018).

4.2.2 Temporal variation of sources

The predominant origin of Pb in PM2.5 was further evidenced by the plotting of Pb isotopic ratios ($^{208}Pb/^{206}Pb$ *vs* $^{207}Pb/^{206}Pb$) from different anthropogenic sources (urban traffic and unleaded gasoline, urban/industrial activities and coal mining) of neighbouring countries (*i.e.,* China, India, Indonesia, Taiwan, Thailand) (Fig. 6, Table S8). Lead in atmospheric particles has been extensively studied in Asian countries over the last two decades and has shown specific isotopic variations depending on the emission source (Bing-Quan et al., 2001; Bollhöfer and Rosman, 2001; Mukai et al., 2001a,b; Zhu et al., 2001; Zheng et al., 2004; Yao et al., 2015; Zhao et al., 2015: Bi et al., 2017). Here, the mixing between three sources is represented by a triangle whose end-members define the Pb isotopic ratios in sources S1, S2 and S3. The end-member S1, less radiogenic than other anthropogenic samples, could represent the geochemical background derived from the Earth's crust (Bollhöfer and Rosman, 2001; Li et al., 2001). However, due to the high heterogeneity of Asian soils and the intensity of anthropogenic activities, the measurement of the geochemical background is uncertain. It is highly probable that natural dusts from long-range transport are contaminated by deposition of anthropogenic emissions (Table 2). The Pb isotopic composition in S1 was compared to ceramic or metals assemblies from neolitic archaeological site in southeast Asian (Pryce et al., 2014). The relics had Pb isotopic signatures close to S1, thus confirming the latter as a natural background. Therefore, Pb isotopic composition in 'natural' soil (S1) were assessed by calculating the intercept between the "coal line" and the "oil line". The Pb isotopic ratios in S2 were associated with those of the Coc Sau coal mine (northern Vietnam; Chifflet et al., 2018) which merges with other Chinese coal mines (the solid green circles specifically representing the southern mines). Finally, the end-member S3 was associated with values from vehicle exhaust emissions in the megacity of Bangkok (Thailand, Bing-Quan et al., 2001) which also merges with those from Chinese unleaded gasoline (Yao et al.,

2015) and Russian oil fields (Mukai et al., 2001b). The orange linear trend is defined with Pb isotopic ratios measured in samples from anthropogenic petroleum-related activities labelled S3 'oil', here after.

The contributions of the three Pb sources in PM2.5 was calculated using a linear mixing model (Fig. 7, Table S9). A low contribution of 'natural' soil (14 ± 11%) and high PM2.5 concentrations (54 ± 30 µg m^{-3}) were observed during the northeast winter monsoon. Conversely, the contribution of 'natural' soil increased sharply (up to 83% on 07/07/2020) with a decrease in PM2.5 concentrations (26 ± 11 µg m^{-3}) during the southeast summer monsoon. In winter, this contribution can be attributed to Asian dust storms, which transport fine soil dust from eastern (or inland) China to northern Vietnam before reaching Hanoi. Locally, the dry climate favours the resuspension of street dust and fine particles from vehicle exhaust (Hein et al., 2002). In addition, during this period, air masses with low vertical mixing favour PM2.5 enrichment (Ngoc et al., 2021), thus decreasing the natural contribution of PM2.5 from long-range transport. Conversely, during the summer monsoon, the increase in natural contribution of PM2.5 can be attributed to both mixing with a cleaner marine airflow and scavenging of local anthropogenic emissions due to a wet climate. The 'oil' contribution (encompassing any use) in PM2.5 remained stable over the sampling period (48 ± 13% during the northeast winter monsoon and 42 ± 17% during the southeast summer monsoon), although the year 2020 is marked by the traffic restrictions imposed by COVID-19 and a possible reduction in fuel consumption in many motorists (*e.g.,* vehicles, buses, trucks *etc.*). In China, almost one third of the cities were in lockdown for several weeks in January and February 2020, resulting in improved local air quality (He et al., 2020; Yuan et al., 2021). Therefore, during this period (winter monsoon), Hanoi may have been less impacted by transboundary oil emissions. In addition, during the summer monsoon, South China Sea winds are expected to decrease the anthropogenic contribution of atmospheric particles in Hanoi (*via* dilution and wet scavenging) which does not seem to be the case for the 'oil' contribution which remains stable over the year. These observations suggest that 'oil' contribution in PM2.5 was mainly of local origin, not influenced by long-range transport from China

or South China Sea. In contrast, coal had a higher contribution in PM2.5 during the northeast winter monsoon (38 ± 13%) than during southeast summer monsoon (26 ± 15%). Despite the rapid development of green energy (wind and solar), CO_2 emissions continue to rise in China. In 2020, the Chinese coal industry emitted 761 Mt CO_2 (*i.e,* 70% of China's total CO_2 emissions) due to the growing demand for electricity (IEA, 2020; https://ourworldindata.org/). In addition, Vietnam has also large coal reserves in the north of the country and the share of coal-fired power generation has increased to 50% by 2020 (https://ember-climate.org/). Therefore, the results show a latent local coal contribution in PM2.5 (about 26%) enriched by Chinese coal emissions (about +12%) in winter.

4.3 Human health risk assessment through exposure to PM2.5

In this study, PM2.5 contain high concentrations of MM, which may constitute a health risk. Therefore, a comprehensive human health risk assessment can provide useful information for public policy management. The hazard quotient (HQ_i) per element could be ranked in the following order: Cr > Pb > Sb > Zn > Cu > Mn > As > Ti > Cd > V > Ni > Al > Co > Hg > U. The cumulative hazard index (HI) was less than 1 (*i.e,* 0.076), suggesting that inhalation of the 15 elements bound to PM2.5 has no chronic influence (Table 3). In addition, the total carcinogenic risk (TCR) was estimated at $1.0\ 10^{-4}$, which suggests that the probability of a person developing cancer by inhalation is low, but would be mainly imputable to Cr.

Other studies on human health risk assessment of PM2.5 in Hanoi estimated risk values similar to our results: HI = 0.13 ± 0.08 and TCR = $1.13\ 10^{-5}$ (Hein et al., 2022), HI = 1.16 and TCR = $9\ 10^{-6}$ (Nguyen et al., 2022) or HI = 0.006 and TCR = $5.5\ 10^{-7}$ (Bui et al., 2022). The differences between HI and TCR values may be explained by the random or incomplete sampling frequency, which were carried out only in winter 2018-2019, in three seasons winter-spring-fall 2020 or in two seasons summer-fall 2020, respectively. However, these studies concluded that Cr and As presented a risk of inhalation exposure. According to the International Agency for Research on Cancer, Cr (Group 1) can induce harmful human health effects. Coal naturally contains large amounts of Cr (Zhang et al., 2004;

Ketris and Yudovich, 2009; Dai et al., 2012) which are transferred to atmospheric particles during combustion processes (Xu et al., 2004b). Consequently, coal mining and combustion could potentially induce human diseases.

Despite risks on human health, Vietnam has significantly increased its use of coal, positioned as the world's tenth largest producer of coal-fired electricity. In 2022, Vietnamese economy grew by 8% with a very large increase in energy use (https://ember-climate.org/). Despite the boom in the deployment of renewables energies, Vietnam faces several challenges (industrial, economic and politic) in its effort to become carbon neutral. A "Just Energy Transition Partnership" plan was signed in 2022 in order to help the country to peak its greenhouse gas emissions by 2030 instead of 2035, limiting its production of coal energy to 30.2 GW instead of 37 GW, and source 47% of its power from renewable energy by 2030 (COP27 climate summit; https://unfccc.int/cop27). This study highlights the need for strict regulatory plans to control hazardous MM emissions by reducing coal combustion. In addition, due to the impact of oil combustion in PM2.5, public policies should encourage conversion to green transport to limit global warming.

5. Conclusion

Our study provided a detailed overview of the annual variation in PM2.5 concentrations in Hanoi (northern Vietnam), evaluated Pb anthropogenic sources and examined the impact of weather conditions on inhaled MM concentrations and related toxic risks.

The annual average PM2.5 concentration (40.2 ± 26.3 µg m^{-3}) was 1.6 and 8.0 times higher than the national and global standards, respectively. In addition, some PM2.5-bound MM (Pb, As, Cd and Cr) had 24-hour maximum concentrations above the annual exposure limits. Chemical ratios (V/Ni, Cd/Pb, Sb/Cd and Al/Ti) presented typical trends indicating the dominance of three emission sources from road traffic, natural soil, and coal uses (mining, combustion). The source contribution was assessed using Pb isotopic ratios ($^{208}Pb/^{206}Pb$ *vs* $^{207}Pb/^{206}Pb$). The oil contribution (encompassing

any petroleum-related activities) to PM2.5 remained stable over the sampling period (November 2019 to December 2020) with an annual average of 45%. In contrast, PM2.5 inputs from soil and coal were impacted by weather conditions. Indeed, 'natural' soil contribution varied between 14 to 83% depending on the winter and summer monsoons, respectively.. Conversely, coal contribution was higher in the winter (38%)than in the summer (26%) monsoon. This phenomenon could be due to the BC emissions (from the incomplete combustion of fossil fuels) coming from both long-range air transport and local emissions. In addition, the human health risk assessment showed that PM2.5-bound MM concentrations obtained in this study have no chronic influence although Cr, Pb and Sb have the highest HQ_i values. The carcinogenic risk is low but mainly imputable to Cr.

In order to discriminate more precisely the black carbon fractions linked to agricultural burning from those linked to the combustion of fossil fuels, a companion paper will cover the study of major inorganic ions (NH_4^+, NO_3^-, SO_4^{2-}, Na^+) and other elements (Ca, K, Mg, P), as well as carbon speciation (OC, EC, sugars).

Supplementary information

The supplementary material related to this article is available online at XXX.

Acknowledgments

The project received financial support from the French (IRD, IRN-SOOT SEA) and Vietnamese (VAST-IMER) research organizations. We thank the MIO "Plateforme Analytique de Chimie des Environnements Marins" (PACEM platform) for laboratory facilities. The authors would like to thank the dedicated efforts of people from Air-o-Sol Platform at IGE for analysing the PM2.5 samples. The

authors are deeply grateful for the thorough and constructive corrections and insightful comments of the anonymous reviewers, who have significantly improved the original manuscript.

References

Bacon, S.N., McDonald, E.V., Amit, R., Enzel, Y., Crouvi, O., 2011. Total suspended particulate matter emissions at high friction velocities from desert landforms. J. Geophys. Res., 116, F03019. https://doi.org/10.1029/2011JF001965.

Balali-Mood, M., Naseri, K., Tahergorabi, Z., Khazdair, M.R., Sadeghi, M., 2021 Toxic mechanisms of five heavy metals: mercury, lead, chromium, cadmium, and arsenic. Front. Pharmacol., 12, 643972. https://doi.org/10.3389/fphar.2021.643972.

Behrooz, R.D., Kaskaoutis, D.G., grivas, G., Mihalopoulos, N., 2021. Human health risk assessment for toxic elements in the extreme ambient dust conditions observed in Sistan, Iran. Chemosphere, 262, 127835. https://doi.org/10.1016/j.chemosphere.2020.127835.

Bi, X.Y., Li, Z.G., Wang, S.X., Zhang, L., Xu, R., Liu, J.L., Yang, H.M., Guo, M.Z., 2017. Lead Isotopic Compositions of Selected Coals, Pb/Zn Ores and Fuels in China and the Application for Source Tracing. Environ. Sci. Technol., 51, 13502-13508. https://doi.org/10.1021/acs.est.7b04119.

Bing-Quan, Z., Yu-Wei, C., Jian-Hua, P., 2001. Lead isotope geochemistry of the urban environment in the Pearl River Delta. App. Geochem., 16, 409-417. https://doi.org/10.1016/S0883-2927(00)00047-0.

Bing-Quan, Z., Yu-Wei, C., Xiang-yang, C., 2002. Application of Pb isotopic mapping to environment evaluation in China. Chem. Speciat. Bioavailab., 14, 49-56. https://doi.org/10.3184/095422902782775335.

Bollhöfer, A., Rosman, K.J.R., 2000. Isotopic source signatures for atmospheric lead: the Southern hemisphere. Geochim. Cosmochim. Acta, 64, 3251-3262. https://doi.org/10.1016/S0016-7037(00)00436-1.

615 Bollhöfer, A, Rosman, K.J.R., 2001. Isotopic source signatures for atmospheric lead: the Northern
616 Hemisphere. Geochim. Cosmochim. Acta, 65, 1727-1740. https://doi.org/10.1016/S0016-
617 7037(00)00630-X.
618 Bui, T.H., Nguyen, D.L., Nguyen, T.P.M., Bui, Q.T., Nguyen, V.D., Mac, V.D., 2022. Chemical
619 characterization, source apportionment, and human health risk assessment of PM2.5 in an
620 urban area in Hanoi, Vietnam. Air Qual. Atmos. Health, 16, 149-163.
621 https://doi.org/10.1007/s11869-022-01266-0.
622 Chen, M., Ma, L.Q., 2001. Comparison of Three Aqua Regia Digestion Methods for Twenty Florida
623 Soils. Soil Sci. Soc. Am. J., 65, 491-499. https://doi.org/10.2136/sssaj2001.652491x.
624 Chen, Y.C., Hsu, C.Y., Lin, S.L., Chang-Chien, G.P., Chen, M.J., Fang, G.C., Chiang, H.C., 2015.
625 Characteristics of Concentrations and Metal Compositions for PM2.5 and PM2.5-10 in Yunlin
626 County, Taiwan during Air Quality Deterioration. Aerosol Air Qual. Res., 15, 2571-2583.
627 https://doi.org/10.4209/aaqr.2015.04.0261.
628 Cheng, I., Al Mamun, A., Zhang, L., 2021. A synthesis review on atmospheric wet deposition of
629 particulate elements: scavenging ratios, solubility, and flux measurements. Environ. Rev., 29,
630 340-353. https://doi.org/10.1139/er-2020-0118.
631 Chifflet, S., Amouroux, D., Bérail, S., Barre, J., Thuoc, T.V., Baltrons, O., Brune, J., Dufour, A., Guinot,
632 B., Mari, X., 2018. Origins and discrimination between local and regional atmospheric pollution
633 in Haiphong (Vietnam), based on metal(loid) concentrations and lead isotopic ratios in PM_{10}.
634 Environ Sci Pollut Res, 25, 26653-26668. https://doi.org./10.1007/s11356-018-2722-7.
635 Chow, J.C., Lowenthal, D.H., Chen, L.W.A., Wang, X., Watson, J.G., 2015. Mass reconstruction
636 methods for PM2.5: a review. Air Qual. Atmos. Health, 8, 243-263.
637 https://doi.org./10.1007/s11869-015-0338-3.
638 Cohen, D.D., Crawford, J., Stelcer, E., Bac, T.V., 2010. Characterisation and source apportionment of
639 fine particulate sources at Hanoi from 2001 to 2008. Atmos. Environ., 44, 320-328.
640 https://doi.org/10.1016/j.atmosenv.2009.10.037.

641 Dai, S., Ren, D., Chou, C.L., Finkelman, R.B., Seredin, V.V., Zhou, Y., 2012. Geochemistry of trace
642 elements in Chinese coals: A review of abundances, genetic types, impacts on human health,
643 and industrial utilization. Int. J. Coal Geol., 94, 3-21.
644 https://doi.org/10.1080/00206814.2017.1405287.
645 Ding, A.J., Huang, X., Nie, W., Sun, J.N., Kerminen, V.-M., Petäjä, T., Su, H., Cheng, Y.F., Yang, X.-Q.,
646 Wang, M.H., Chi, X.G., Wang, J.P., Virkkula, A., Guo, W.D., Yuan, J., Wang, S.Y., Zhang, R.J., Wu,
647 Y.F., Song, Y., Zhu, T., Zilitinkevich, S., Kulmala, M., Fu, C.B., 2016. Enhanced haze pollution by
648 black carbon in megacities in China. Geophys. Res. Lett., 43.
649 https://doi.org/10.1002/2016GL067745.
650 Draxler, R.R., Stunder, B., Rolph, G., Stein, A., Taylor, A., Zinn, S., Loughner, C., Crawford, A., 2022.
651 HYSPLIT User's Guide. Version 5.2, Last revision: Jan 2022.
652 https://www.arl.noaa.gov/documents/reports/hysplit_user_guide.pdf.
653 Duan, X., Yan, Y., Li, R., Deng, M., Hu, D., Peng, L., 2021. Seasonal variations, source apportionment,
654 and health risk assessment of trace metals in PM2.5 in the typical industrial city of Changzhi,
655 China. Atmos. Pollut. Res., 12, 365-374. https://doi.org/10.1016/j.apr.2020.09.017.
656 Duc, H.N., Azzi, M., Zhang, Y., Kirkwood, J., White, S., Trieu, T., Riley, M., Salter, D., Chang, L.T.C.,
657 Capnerhurst, J., Ho, J., Gunashanhar, G., Monk, K., 2023. Black Carbon Emissions, Transport
658 and Effect on Radiation Forcing Modelling during the Summer 2019-2020 Wildfires in
659 Southeast Australia. Atmosphere, 14, 699. https://doi.org/10.3390/atmos14040699.
660 Finlayson-Pitts, B.J., Wingen, L.M., Perraud, V., Ezzll, M.J., 2020. Open questions on the chemical
661 composition of airborne particles. Commun. Chem., 3, 108. https://doi.org/10.1038/s42004-
662 020-00347-4.
663 Font, A., de Hoogh, K., Leal-Sanchez, M., Ashworth, D.C., Brown, R.J.C., Hansell, A.L., Fuller, G.W.,
664 2015. Using metal ratios to detect emissions from municipal waste incinerators in ambient air
665 pollution data. Atmos. Environ., 113, 177-186.
666 http://dx.doi.org/10.1016/j.atmosenv.2015.05.002.

667 Fuzzi, S., Baltensperger, U., Carslaw, K., Decesari, S., Denier van der Gon, H., Facchini, M. C., Fowler,
668 D., Koren, I., Langford, B., Lohmann, U., Nemitz, E., Pandis, S., Riipinen, I., Rudich, Y., Schaap,
669 M., Slowik, J. G., Spracklen, D. V., Vignati, E., Wild, M., Williams, M., and Gilardoni, S., 2015.
670 Particulate matter, air quality and climate: lessons learned and future needs. Atmos. Chem.
671 Phys., 15, 8217-8299. https://doi.org/10.5194/acp-15-8217-2015.
672 Gieré, R., Querol, X., 2010. Solid Particulate Matter in the Atmosphere. Elements, 6, 215-222.
673 https://doi.org/10.2113/gselements.6.4.215.
674 Gilbert, R.O., 1987. Statistical Methods for Environmental Pollution Monitoring. John Wiley & Sons,
675 Inc., New York, pp. 177-185. ISBN: 978-0-471-28878-7.
676 Guo, F., Tang, M., Wang, X., Yu, Z., Wei, F., Zhang, X., Jin, M., Wang, J., Xu, D., Chen, Z., Chen, K.,2022.
677 Characteristics, sources, and health risks of trace metals in PM2.5. Atmos. Environ., 289,
678 119314. https://doi.org/10.1016/j.atmosenv.2022.119314.
679 Guo, S., Tao, X., Liang, L., 2023. Exploring Natural and Anthropogenic Drivers of $PM_{2.5}$ Concentrations
680 Based on Random Forest Model: Beijing–Tianjin–Hebei Urban Agglomeration, China.
681 Atmosphere, 14, 381. https://doi.org/10.3390/atmos14020381.
682 Hai, C.D., Kim Oanh, N.T., 2013. Effects of local, regional meteorology and emission sources on mass
683 and compositions of particulate matter in Hanoi. Atmos. Environ. 78, 105-112.
684 https://doi.org/10.1016/j.atmosenv.2012.05.006.
685 Hao, Y., Meng, X., Yu, X., Lei, M., Li, W., Shi, F., Yang, W., Zhang, S., Xie, S., 2018. Characteristics of
686 trace elements in PM2.5 and PM10 of Chifeng, northeast China: Insights into spatiotemporal
687 variations and sources. Atmos. Res., 213, 550-561.
688 https://doi.org/10.1016/j.atmosres.2018.07.006.
689 He, G., Pan, Y., Tanaka, T., 2020. The short-term impacts of COVID-19 lockdown on urban air
690 pollution in China. Nat. Sustain., 3, 1005–1011. https://doi.org/10.1038/s41893-020-0581-y.
691 Henry R.C., Lewis C.W., Hopke P.K., Williamson H.J., 1984. Review of receptor model fundamentals.
692 Atmos. Environ., 18, 1507-1515. https://doi.org/10.1016/0004-6981(84)90375-5.

693 Hien, P.D., Bac, V.T., Tham, H.C., Nhan, D.D., Vinh, L.D., 2002. Influence of meteorological conditions
694 on $PM_{2.5}$ and PM_{10} concentrations during the monsoon season in Hanoi, Vietnam. Atmos.
695 Environ., 36, 3473–3484. https://doi.org/10.1016/S1352-2310(02)00295-9.
696 Hien, P.D., Men, N.T., Tan, P.M., Hangartner, M., 2020. Impact of urban expansion on the air
697 pollution landscape: a case study of Hanoi, Vietnam. Sci. Total Environ., 702, 134635.
698 https://doi.org/10.1016/j.scitotenv.2019.134635.
699 Hien, T.T., Chi N.C.T., Huy, D.H., Le, H.A., Oram, D.E., Forster, G.L., Mills, G.P., Baker, A.R., 2022.
700 Soluble trace metals associated with atmospheric fine particulate matter in the two most
701 populous cities in Vietnam. Atmos. Environ., 15, 100178.
702 https://doi.org/10.1016/j.aeaoa.2022.100178.
703 Hopke, P. K., 2000. A guide to positive matrix factorization. In: Workshop on UNMIX and PMF as
704 applied to PM2, 5, pp 600.
705 Hopke, P.K., Cohen, D.D., Begum, B.A., Biswas, S.K., Ni, B., Pandit, G.G., Santoso, M., Chung, Y.-S.,
706 Davy, P., Markwitz, A., Waheed, S., Siddique, N., Santos, F.L., Pabroa, P.C.B., Seneviratne,
707 M.C.S., Wimolwattanapun, W., Bunprapob, S., Vuong, T.B., Duy Hien, P., Markowicz, A., 2008.
708 Urban air quality in the Asian region. Sci. Total Environ. 404, 103–112.
709 https://doi.org/10.1016/j.scitotenv.2008.05.039
710 Hopke, P.K., Cohen, D.D., 2011. Application of receptor modeling methods. Atmos. Pollut. Res., 2,
711 122-125. https://doi.org/10.5094/APR.2011.016.
712 Hsu, S.C., Liu, S.C., Jeng, W.L., Lin, F.J., Huang, Y.T., Lung, S.C.C., Liu, T.H., Tu, J.Y., 2005. Variations of
713 Cd/Pb and Zn/Pb ratios in Taipei aerosols reflecting long-range transport or local pollution
714 emissions. Sci. Tot. Environ., 347, 111-121. https://doi.org/10.1016/j.scitotenv.2004.12.021.
715 Hu, X., Zhang, Y., Ding, Z., Wang, T., Lian, H., Sun, Y., Wu, J., 2012. Bioaccessibility and health risk of
716 arsenic and heavy metals (Cd, Co, Cr, Cu, Ni, Pb, Zn and Mn) in TSP and PM2.5 in Nanjing,
717 China. Atmos. Environ., 57, 146–152. https://doi.org/10.1016/j.atmosenv.2012.04.056.

718 Hu, K., Zha, D., Liu, D., Ding, S., Tian, P., Yu, C., Zhou, W., Huang, M., Ding, D., 2020. Estimating
719 radiative impacts of black carbon associated with mixing state in the lower atmosphere over
720 the northern North China Plain. Chemosphere, 252, 126455.
721 https://doi.org/10.1016/j.chemosphere.2020.126455.
722 Huu, D.N., Ngoc, V.N., 2021. Analysis study of current transportation status in Vietnam's urban traffic
723 and the transition to electric two-wheelers mobility. Sustainability, 13, 5577.
724 Huy, L.N., Kim Oanh, N.T., 2017. Assessment of national emissions of air pollutants and climate
725 forcers from thermal power plants and industrial activities in Vietnam. Atmos. Pollut. Res., 8,
726 503-513. https://doi.org/10.1016/j.apr.2016.12.007.
727 IEA (International Energy Agency), 2020. Energy Technology Perspectives 2020, IEA, Paris 400 p.
728 IARC, 2023. Monographs on the Evaluation of Carcinogenic Risks to Humans Volume 1-133.
729 https://monographs.iarc.who.int/agents-classified-by-the-iarc/.
730 Jaishankar, M., Tseten, T., Anbalagan, N., Mathew, B.B., Beeregowda, K.N., 2014. Toxicity,
731 mechanism and health effects of some heavy metals. Interdiscip. Toxicol., 7, 60-72.
732 https://doi.org/10.2478/intox-2014-0009.
733 Jaffrezo, J.L., Colin, J.L., 1988. Rain-aerosol coupling in urban area: Scavenging ratio measurement
734 and identification of some transfer processes. Atmos. Environ., 22, 929-935.
735 https://doi.org/10.1016/0004-6981(88)90270-3.
736 Janssen, N.A.H., Hoek, G., Simic-Lawson, M., Fischer, P., van Bree, L., ten Brink, H., Keuken, M.,
737 Atkinson, R.W., Anderson, H.R., Brunekreef, B., Cassee, F.R., 2011. Black Carbon as an
738 Additional Indicator of the Adverse Health Effects of Airborne Particles Compared with PM_{10}
739 and $PM_{2.5}$. Environmental Health Perspectives, 119, 12. https://doi.org/10.1289/ehp.1003369.
740 Ketris, M.P.; Yudovich, Ya.E., 2009. Estimation of clarkes for carbonaceous biotithes: World averages
741 for trace element contents in black shales and coals. Int. J. Coal Geol., 78, 135-148.
742 https://doi.org/10.1016/j.coal.2009.01.002.

743 Kikuchi, T., Hai, H.T., Tanaka, S., 2010. Characterization of heavy metal contamination from their
744 spatial distribution in sediment of an urban lake of Hanoi, Vietnam. J. Water Environ. Technol.,
745 8, 111-123. https://doi.org/10.2965/jwet.2010.111.
746 Kim, K.H., Choi, G.H., Kang, C.H., Lee, J.H., Kim, J.Y., Youn, Y.H., Lee, S.R., 2003. The chemical
747 composition of fine and coarse particles in relation with the Asian Dust events. Atmos.
748 Environ., 37, 753-765. https://doi.org/10.1016/S1352-2310(02)00954-8.
749 Komárek, M., Ettler, V., Chrastny, V., Milhaljevic, M., 2008. Lead isotopes in environmental sciences:
750 a review. Environ. Int., 34, 562-577. https://doi.org/10.1016/j.envint.2007.10.005.
751 Laskin, A., Moffet, R.C., Gilles, M.K., 2019. Chemical imaging of atmospheric particles. Acc. Chem.
752 Res., 52, 3419-3431. https://doi.org/10.1021/acs.accounts.9b00396.
753 Lasko, K., Vadrevu, K., 2018. Improved rice residue burning emissions estimates: Accounting for
754 practice-specific emission factors in air pollution assessments of Vietnam. Environ. Pollut., 236,
755 795-806. https://doi.org/10.1016/j.envpol.2018.01.098.
756 Lelieveld, J., Pozzer, A., Pöschl, U., Fnais, M., Haines, A., Münzel, T., 2020. Loss of life expectancy from
757 air pollution compared to other risk factors: a worldwide perspective. Cardiovascular research,
758 116, 1910-1917. https://doi.org/10.1093/cvr/cvaa025.
759 Le, H.A., Phuong, D.M., Linh, L.T., 2020. Emission inventories of rice straw open burning in the Red
760 River Delta of Vietnam: evaluation of the potential of satellite data. Environ. Pollut., 260,
761 113972 https://doi.org/10.1016/j.envpol.2020.113972.
762 Lee, S.W., Pomalis, R., Kan, B., 2000. A new methodology for source characterization of oil
763 combustion particulate matter. Fuel Process. Technol., 65-66, 189-202.
764 https://doi.org/10.1016/S0378-3820(99)00086-7.
765 Li, J., Okin, G.S., Epstein, H.E., 2009. Effects of enhanced wind erosion on surface soil texture and
766 characteristics of windblown sediments. J. Geophys. Res., 114, G02003.
767 https://doi.org/10.1029/2008JG000903.

Li, F., Yan, J., Wei, Y., Zeng, J., Wang, X., Chen, X., Zhang, C., Li, W., Chen, M., Lü, G., 2021. PM2.5-bound heavy metals from the major cities in China: Spatiotemporal distribution, fuzzy exposure assessment and health risk management. J. Clean. Prod., 286, 124967. https://doi.org/10.1016/j.jclepro.2020.124967.

Li, J., Lin, Y., Nguyen, X., Zhuang, X., Li, B., Querol, X., Moreno, N., Cordoba, P., 2023. Enrichment of strategic metals in the Upper Triassic coal from the Nui Hong open-pit mine, Thai Nguyen Coalfield, NE Vietnam. Ore Geol. Rev., 153, 105301. https://doi.org/10.1016/j.oregeorev.2023.105301.

Liao, K., Zhang, J., Chen, Y., Lu, X., Fung, J.C.H., Ying, Q., Yu, J.Z., 2023. Regional source apportionment of trace metals in fine particulate matter using an observation-constrained hybrid model. Clim. Atmos. Sci., 6, 65. https://doi.org/10.1038/s41612-023-00393-4.

Ly, B.T., Matsumi, Y., Vu, T.V., Sekiguchi, K., Nguyen, T.T., Pham, C.T., Nghiem, T.D., Ngo, I.H., Kurotsuchi, Y., Nguyen, T.H., Nakayama, T., 2021. The effects of meteorological conditions and long-range transport on PM2.5 levels in Hanoi revealed from multi-site measurement using compact sensors and machine learning approach. J. Aerosol Sci., 152, 105716. https://doi.org/10.1016/j.jaerosci.2020.105716.

Makkonen, U., Vestenius, M., Huy, L.N., Anh, N.T.N., Linh, P.T.V., Thuy, P.T., Phuong, H.T.M., Nguyen, H., Thuy, L.T., Aurela, M., Hellén, H., Loven, K., Kouznetsov, R., Kyllönen, K., Teinilä, K., Kim Oanh, N.T., 2023. Chemical composition and potential sources of PM2.5 in Hanoi. Atmos. Environ., 299, 119650. https://doi.org/10.1016/j.atmosenv.2023.119650.

Mazzei, F., D'Alessandro, A., Lucarelli, F., Nava, S., Prati, P., Valli, G., Vecchi, R., 2008. Characterization of particulate matter sources in an urban environment. Sci. Tot. Environ., 401, 81-89. https://doi.org/10.1016/j.scitotenv.2008.03.008.

McNeill, J., Snider, G., Weagle, C.L., Walsh, B., Bissonnette, P., Stone, E., Abboud, I., Akoshile, C., Anh, N.X., Balasubramanian, R., Brook, J.R., Coburn, C., Cohen, A., Dong, J., Gagnon, G., Garland, R.M., He, K., Holben, B.N., Kahn, R., Kim, J.S., Lagrosas, N., Lestari, P., Liu, Y., Jeba, F., Joy, K.J.,

794 Martins, J.V., Misra, A., Norford, L.K., Quel, E.J., Salam, A., Schichtel, B., Tripathi, S. N., Wang,
795 C., Zhang, Q., Brauer, M., Gibson, M.D., Rudich, Y., Martin, R.V., 2020. Large global variations in
796 measured airborne metal concentrations driven by anthropogenic sources. Sci Rep., 10, 21817.
797 https://doi.org/10.1038/s41598-020-78789-y.
798 Mitra, S., Chakraborty, A.J., Tareq, A.M., Emran, T.B., Nainu, F., Khusro, A., Idris, A.M., Khandaker,
799 M.U., Osman, H., Alhumaydhi, F.A., Simal-Gandara, J., 2022. Impact of heavy metals on the
800 environment and human health: Novel therapeutic insights to counter the toxicity. J. King Saud
801 Univ. Sci., 34, 101865. https://doi.org/10.1016/j.jksus.2022.101865
802 Monna, F., Lancelot, J., Croudace, I.W., Cundy, A.B., Lewis, J.T., 1997. Pb isotopic composition of
803 airborne particulate material from France and the Southern United Kingdom: implications for
804 Pb pollution sources in urban areas. Environ. Sci. Technol., 31, 2277-2286.
805 https://doi.org/10.1021/es960870+.
806 Mukai, H., Tanaka, A., Fujii, T., Zeng, Y., Hong, Y., Tang, J., Guo, S., Xue, H., Sun, Z., Zhou, J., Xue, D.,
807 Zhao, J., Zhai, G., Gu, J., Zhai, P., 2001a. Regional characteristics of sulphur and lead isotope
808 ratios in the atmosphere at several Chinese urban sites. Environ. Sci. Technol., 35, 1064-1071.
809 https://doi.org/10.1021/es001399u.
810 Mukai, H., Machida, T., Tanaka, A., Vera, Y.P., Uematsu, M., 2001b. Lead isotope ratios in the urban
811 air of eastern and central Russia. Atmos. Environ., 35, 2783-2793.
812 https://doi.org/10.1016/S1352-2310(00)00341-1.
813 Ngoc, B.A.P., Delbarre, H., Deboudt, K., Dieudonné, E., Tran, D.N., Thanh, S.L., Pelon, J., Ravetta, F.,
814 2021. Key factors explaining severe air pollution episodes in Hanoi during 2019 winter season.
815 Atmos. Pollut. Res., 12, 101068. https://doi.org/10.1016/j.apr.2021.101068.
816 Ngu, N.D., Hieu, N.T., 2004. Climate and Climate Resources of Vietnam (Khi Hau Va Tai Nguyen Khi
817 Hau, Vietnam). IHA. Agriculture Publisher, Hanoi, Vietnam.

818 Nguyen, T.H., Nagashima, T., Doan, Q.V., 2020. Air Quality Modelling Study on the Controlling Factors
819 of Fine Particulate Matter ($PM_{2.5}$) in Hanoi: A Case Study in December 2010. Atmosphere, 11,
820 733. https://doi.org/10.3390/atmos11070733.
821 Nguyen, T.P.M., Bui, T.H., Nguyen, M.K., Ta, T.N., Tran, T.M.H., Nguyen, Y.N., Nguyen, T.H., 2022.
822 Assessing pollution characteristics and human health risk of exposure to PM2.5-bound trace
823 metals in a suburban area in Hanoi, Vietnam. Human and Ecological Risk Assessment: An
824 International Journal, 28, 433-454. https://doi.org/10.1080/10807039.2022.2056872.
825 OEHHA, 2019. California department of toxic substances control (DTSC). Human and ecological risk
826 office (HERO). Human health risk assessment (HHRA). HERO HHRA Note n°10, 25 Febuary
827 2019. https://dtsc.ca.gov/wp-content/uploads/sites/31/2019/02/HHRA-Note-10-2019-02-
828 25.pdf
829 Okuda, T., Kato, J., Mori, J., Tenmoku, M., Suda, Y., Tanaka, S., He, K., Ma, Y., Yang, F., Yu, X., Duan, F.,
830 Lei, Y., 2004. Daily concentrations of trace metals in aerosols in Beijing, China, determined by
831 using inductively coupled plasma mass spectrometry equipped with laser ablation analysis, and
832 source identification of aerosols. Sci. Tot. Environ., 330, 145-158.
833 https://doi.org/10.1016/j.scitotenv.2004.04.010.
834 Oravisjarvi, K., Timonen, K.L., Wiikinkoski, T., Ruuskanen, A.R., Heinanen, K., Ruuskanen, J., 2003.
835 Source contributions to $PM_{2.5}$ particles in the urban air of a town situated close to a steel
836 works. Atmos. Environ., 37, 1013-1022. https://doi.org/10.1016/S1352-2310(02)01048-8.
837 Ortega, G.S., Pécheyran, C., Bérail, S., Donard, O.F., 2012. A fit-for purpose procedure for lead
838 isotopic ratio determination in crude oil, asphaltene and kerogen samples by MC-ICP-MS. J.
839 Anal. At. Spectrom., 27, 1447-1456. https://doi.org/10.1039/C2JA30143A.
840 Paatero, P., Tapper, U., 1994. Positive Matrix Factorisation: a non-negative factor model with optimal
841 utilisation of error estimates of data values. Environmetrics, 5, 111-126.
842 https://doi.org/10.1002/env.3170050203.

Pacyna, J.M., Pacyna, E.G., 2001. An assessment of global and regional emissions of trace metals to the atmosphere from anthropogenic sources worldwide. Environ. Rev., 9, 269-298. https://doi.org/10.1139/a01-012.

Pacyna, E.G., Pacyna, J.M., Fudala, J., Strzelecka-Jastrzab, E., Hlawiczka, S., Panasiuk, D., Nitter, S., Pregger, T., Pfeiffer, H., Friedrich, R., 2007. Current and future emissions of selected heavy metals to the atmosphere from anthropogenic sources in Europe. Atmos. Environ., 41, 8557-8566. https://doi.org/10.1016/j.atmosenv.2007.07.040.

Palleschi, S., Rossi, B., Armiento, G., Montereali, M.R., Nardi, E., Tagliani, S.M., Inglessis, M., Gianfagna, A., Silvestroni, L., 2018. Toxicity of the readily leachable fraction of urban PM2.5 to human lung epithelial cells: role of soluble metals. Chemosphere, 196, 35–44. https://doi.org/10.1016/j.chemosphere.2017.12.147.

Pan, Y.P., Wang, Y.S., 2014. Atmospheric wet and dry deposition of trace elements at ten sites in Northern China. Atmos. Chem. Phys. Discuss., 14, 20647-20676. https://doi.org/10.5194/acp-15-951-2015.

Pant, P., Harrison, R.M., 2012. Critical review of receptor modelling for particulate matter: A case study of India. Atmos. Environ., 49, 1-12. https://doi.org/10.1016/j.atmosenv.2011.11.060.

Pekney, N.J., Davidson, C.L., 2005. Determination of trace elements in ambient aerosol samples. Anal. Chim. Acta, 540, 269-277. https://doi.org/10.1016/j.aca.2005.03.065.

Petäjä, T., Järvi, L., Kerminen, V.M., Ding, A.J., Sun, J.N., Nie, W., Kujansuu, J., Virkkula, A., Yang, X.Q., Fu, C.B., Zilitinkevich, S., Kulmala, M., 2016. Enhanced air pollution via aerosol-boundary layer feedback in China. Sci. Rep., 6, 18998. https://doi.org/10.1038/srep18998 .

Pope, C.A., Brook, R.D., Burnett, R.T., Dockery, D.W., 2011. How is cardiovascular disease mortality risk affected by duration and intensity of fine particulate matter exposure? An integration of the epidemiologic evidence. Air Qual. Atmos. Health, 4, 5-14. https://doi.org/10.1007/s11869-010-0082-7.

Pryce, T.O., Baron, S., Bellina, B.H.M., Bellwood, P.S., Chang, N., Chattopadhyay, P., Dizon, E., Glover, I.C., Hamilton, E., Higham, C.F.W., Kyaw, A.A, Laychour, V., Natapintu, S., Nguyen, V., Pautreau, J.P., Pernicka, E., Pigott, V.C., Pollard, M., Pottier, C., Reinecke, A., Sayavongkhamdy, T., Souksavatdy, V., White, J., 2014. More questions than answers: the Southeast Asian Lead Isotope Project 2009–2012. J. Archaeol. Sci., 42, 273-294. https://doi.org/10.1016/j.jas.2013.08.024.

Quang, T.N., Hue, N.T., Dat, M.V., Tran, L.K., Phi, T.H., Morawska, L., Thai, P.K., 2021. Motorcyclists have much higher exposure to black carbon compared to other commuters in traffic of Hanoi, Vietnam. Atmos. Environ., 245, 118029. https://doi.org/10.1016/j.atmosenv.2020.118029.

Rafiee, A., Delgado-Saborit, J.M., D.Sly, P., Qu´emerais, B., Hashemi, F., Akbari, S., Hoseini, M., 2020. Environmental chronic exposure to metals and effects on attention and executive function in the general population. Sci. Total Environ., 705, 135911. https://doi.org/10.1016/j.scitotenv.2019.135911.

Rolph, G., Stein, A., Stunder, B., 2017. Real-time environmental applications and display system: ready. Environ. Model. Software, 95, 210–228. https://doi.org/10.1016/j. envsoft.2017.06.025.

Roy, D., Singh, G., Seo, Y.C., 2019. Carcinogenic and non-carcinogenic risks from PM10-and PM2.5-bound metals in a critically polluted coal mining area. Atmos. Pollut. Res., 10, 1964–1975. https://doi.org/10.1016/j.apr.2019.09.002.

Roy, S., Lam, Y.F., Hung, N.T., Chan, J.C.L., Fu, J.S., 2021. Development of 2015 Vietnam emission inventory for power generation units. Atmos. Environ., 247, 118042 https://doi.org/10.1016/j.atmosenv.2020.118042.

Sakundoo, P., Thonglua, T., Sangkham, S., Jirapornkul, C., Limmongkon, Y., Daduang, S., Tessiri, T., Rayubkul, J., Thongtip, S., Maneenin, N., Pimonsree, S., 2022. Human health risk assessment of PM2.5-bound heavy metal of anthropogenic sources in the Khon Kaen Province of Northeast Thailand. Heyliyon, 8, e09572. https://doi.org/10.1016/j.heliyon.2022.e09572.

Seinfeld, J.H., 2014. Tropospheric chemistry and composition: aerosols/particles. In: North, G.R., Pyle, J., Zhang, F. (Eds.), Encyclopedia of Atmospheric Sciences, Second edition. Academic Press, Oxford, pp. 182-187. https://doi.org/10.1016/b978-0-12-382225-3.00438-2.

Shen, Z.X., Cao, J.J., Arimoto, R., Zhang, R.J., Jie, D.M., Zhu, C.S., 2007. Chemical composition and source characterization of spring aerosol over Horqin sand land in northeastern China. J. Geophys. Res.: Atmos., 112, D14. https://doi.org/10.1029/2006JD007991.

Soetrisno, F.N., Delgado-Saborit, J.M., 2020. Chronic exposure to heavy metals from informal e-waste recycling plants and children's attention, executive function and academic performance. Sci. Total Environ., 717, 137099. https://doi.org/10.1016/j.scitotenv.2020.137099.

Stacey, J.S., Kramers, J.D., 1975. Approximation of terrestrial lead isotope evolution by a two-stage model. Earth Planet. Sci. Lett., 26, 207-221. https://doi.org/10.1016/0012-821X(75)90088-6.

Stanaway, J.D., Afshin, A., Gakidou, E., Lim, S.S., Abate, D., Abate, K.H., Abbafati, C., et al., 2018. Global, regional, and national comparative risk assessment of 84 behavioural, environmental and occupational, and metabolic risks or clusters of risks for 195 countries and territories, 1990–2017: A systematic analysis for the Global Burden of Disease Study 2017. Lancet, 392, 1923-1994. https://doi.org/10.1016/S0140-6736(18)32225-6.

Stein, A.F., Draxler, R.R., Rolph, G.D., Stunder, B.J.B., Cohen, M.D., Ngan, F., 2015. NOAA's HYSPLIT atmospheric transport and dispersion modeling system. Bull. Am. Meteorol. Soc., 96, 2059–2077. https://doi.org/10.1175/BAMS-D-14-00110.1.

Sun, R., Liu, G., Zheng, L., Chou, C.L., 2010. Geochemistry of trace elements in coals from the Zhuji Mine, Huainan Coalfield, Anhui, China. Int. J. Coal Geol., 81, 81-96. https://doi.org/10.1016/j.coal.2009.12.001.

Sun R., Sonke, J.E., Heimbürger, L.E., Belkin, H.E., Liu, G., Shome, D., Cukrowska, E., Liousse, C., Pokrovsky, O.S., Streets, D.G., 2014. Mercury Stable Isotope Signatures of World Coal Deposits and Historical Coal Combustion Emissions. Environ. Sci. Technol., 48, 7660-7668. https://doi.org/10.1021/es501208a.

Tang, Q., Liu, G., Zhou, C., Sun, R., 2013. Distribution of trace elements in feed coal and combustion residues from two coal-fired power plants at Huainan, Anhui, China. Fuel, 107, 315-322. https://doi.org/10.1016/j.fuel.2013.01.009.

Thorpe, A., Harrison, R.M., 2008. Sources and properties of non-exhaust particulate matter from road traffic: a review. Sci. Tot. Environ., 400, 270-282. https://doi.org/10.1016/j.scitotenv.2008.06.007.

Tian, H., Zhou, J., Zhu, C., Zhao, D., Gao, J., Hao, J., He, M., Liu, K., Wang, K., Hua, S., 2014. A Comprehensive Global Inventory of Atmospheric Antimony Emissions from Anthropogenic Activities, 1995-2010. Environ. Sci. Technol., 48, 10235-10241. https://doi.org/10.1021/es405817u.

US. EPA, 1996. Method 3050B: Acid Digestion of Sediments, Sludges, and Soils, Revision 2. Washington, DC.

US EPA, 2005. Aging and toxic response: issues relevant to risk assessment. EPA/600/P-03/004A.

US EPA, 2009. Risk assessment guidance for superfund. Volume I: Human health evaluation manual (Part F, supplemental guidance for inhalation risk assessment). EPA-540-R-070-002, OSWER 9285.7-82.

US EPA, 2013. Reference method for the determination of fine particulate matter as PM 2.5 in the atmosphere. 40 CRF 50.18. Appendix L.

Varrica, D., Bardelli, F., Dongarrà, G., Tamburo, E., 2013. Speciation of Sb in airborne particulate matter, vehicle brake linings, and brake pad wear residues. Atmos. Environ., 64, 18–24. https:/doi.org/10.1016/j.atmosenv.2012.08.067.

Vithanage, M., Bandara, P.C., Novo, L.A.B., Kumar, A., Ambade, B., Naveendrakumar, G., Ranagalage, M., Magana-Arachchi, D.N., 2022. Deposition of trace metals associated with atmospheric particulate matter: Environmental fate and health risk assessment. Chemosphere, 303, 135051. https://doi.org/10.1016/j.chemosphere.2022.135051.

Vo, L.H.T., Yoneda, M., Nghiem, T.D., Shimada, Y., Van, D.H., Nguyen, T.H.T., Nguyen, T.T., 2022. Indoor PM0.1 and PM2.5 in Hanoi: Chemical characterization, source identification, and health risk assessment. Atmos. Pollut. Res., 13, 101324. https://doi.org/10.1016/j.apr.2022.101324.

Vuong, Q.T., Bac, V.T., Thang, P.Q., Park, M.K., Choi, S.D., 2023. Trace element characterization and source identification of particulate matter of different sizes in Hanoi, Vietnam. Urban Climate, 48, 101408. https://doi.org/10.1016/j.uclim.2023.101408.

Wang, X., Dickinson, R.E., Su, L., Zhou, C., Wang, K., 2018. PM2.5 pollution in China and how it has been exacerbated by terrain and meteorological conditions. Bull. Am. Meteorol. Soc., 99, 105-119. https://doi:10.1175/BAMS-D-16-0301.1.

Wedepohl, K.H., 1995.The composition of the continental crust. Geochim. Cosmochim. Acta, 59, 217-1232. http://dx.doi.org/10.1016/0016-7037(95)00038-2.

Wilcox, E.M., Thomas, R.M., Praveen, P.S., Ramanathan, V., 2016. Black carbon solar absorption suppresses turbulence in the atmospheric boundary layer. PNAS, 113, 11794-11799. https://doi.org/10.1073/pnas.1525746113.

Witkowska, D., Słowik, J., Chilicka, K., 2021. Heavy metals and human health: possible exposure pathways and the competition for protein binding sites. Molecules, 26, 6060. doi: 10.3390/molecules26196060. https://doi.org/10.3390/molecules26196060.

World Health Organization, 2021. WHO global air quality guidelines: particulate matter (PM2.5 and PM10), ozone, nitrogen dioxide, sulfur dioxide and carbon monoxide. World Health Organization. https://apps.who.int/iris/handle/10665/345329.

Xing, Y.F., Xu, Y.H., Shi, M.H., Lian, Y.X.,2016. The impact of PM2.5 on the human respiratory system. J. Thorac. Dis., 8, E69-E74. https://doi.org/10.3978/j.issn.2072-1439.2016.01.19.

Xu, J., Bergin, M.H., Greenwald, R., Schauer, J.J., Shafer, M.M., Jaffrezo, J.L., Aymoz, G., 2004a. Aerosol chemical, physical, and radiative characteristics near a desert source region of

969 northwest China during ACE-Asia. J. Geophys. Res.: Atmos., 109, D19.
970 https://doi.org/10.1029/2003JD004239.
971 Xu, M., Yan, R., Zheng, C., Qiao, Y., Han, J., Sheng, C., 2004b. Status of trace element emission in a
972 coal combustion process: a review. Fuel Process. Technol., 85, 215-237.
973 https://doi.org/10.1016/S0378-3820(03)00174-7.
974 Xu, H.M., He, K.L., Feng, R., Shen, Z.X., Cao, J.J., Liu, S.X., Ho, K.F., Huang, R.J., Guinot, B., Wang, Q.Y.,
975 Zhou, J.M., Shen, M.X., Xiao, S., Zhou, B.H., Sonke, J.E., 2020. Metallic elements and Pb
976 isotopes in $PM_{2.5}$ in three Chinese typical megacities: spatial distribution and source
977 apportionment. Environ. Sci., 22, 1718-1730. https://doi.org/10.1039/d0em00174k.
978 Yang, X., Wang, T., Xia, M., Gao, X., Li, Q., Zhang, N., Yuan, G., Lee, S., Wang, X., Xue, L., Yang, L.,
979 Wang, W., 2018. Abundance and origin of fine particulate chloride in continental China. Sci.
980 Total Environ., 624, 1041-1051. https://doi.org/10.1016/j. scitotenv.2017.12.205.
981 Yao, P.H., Shyu, G.S., Chang, Y.F., Chou, Y.C., Shen, C.C., Chou, C.S., Chang, T.K., 2015. Lead isotope
982 characterization of petroleum fuels in Taipei, Taiwan. Int. J. Environ. Res. Public Health, 12,
983 4602-4616. https://doi.org/10.3390/ijerph120504602.
984 Yuan, Q., Qi, B., Hu, D., Wang, J., Zhang, J., Yang, H., Zhang, S., Liu, L., Xu, L., Li, W., 2021.
985 Spatiotemporal variations and reduction of air pollutants during the COVID-19 pandemic in a
986 megacity of Yangtze River Delta in China. Sci. Total Environ., 751, 141820
987 https://doi.org/10.1016/j.scitotenv.2020.141820.
988 Zhang, J., Ren, D., Zhu, Y., Chou, C.L., Zeng, R., Zheng, B., 2004. Mineral matter and potentially
989 hazardous trace elements in coal from Qianxi Fault Depression Area in southwestern Guizhou,
990 China. Int. J. Coal Geol., 57, 49-61. https://doi.org/10.1016/j.coal.2003.07.001.
991 Zhang, X., Eto, Y., Aikawa, M., 2021. Risk assessment and management of PM2.5-bound heavy metals
992 in the urban area of Kitakyushu, Japan. Sci. Tot. Environ., 795, 148748.
993 https://doi.org/10.1016/j.scitotenv.2021.148748.

Zhao, Z.Q., Zhang, W., Li, X.D., Yang, Z., Zheng, H.Y., Ding, H., Wang, Q.L., Xiao, J., Fu, P.Q., 2015. Atmospheric lead in urban Guiyang, Southwest China: Isotopic source signatures. Atmos. Environ., 115, 163-169. https://doi.org/10.1016/j.atmosenv.2015.05.049.

Zheng, J., Tan, M., Yasuyuki, S., Atsushi, T., Li, Y., Zhang, G., Zhang, Y., Shan, Z., 2004. Characteristics of lead isotope ratios and elemental concentrations in PM_{10} fraction of airborne particulate matter in Shanghai after the phase-out lead gasoline. Atmos. Environ., 38, 1191-1200. https://doi.org/10.1016/j.atmosenv.2003.11.004.

Zhou, B., Liu, D., Yan, W., 2021. A Simple New Method for Calculating Precipitation Scavenging Effect on Particulate Matter: Based on Five-Year Data in Eastern China. Atmos., 12, 759, https://doi.org/10.3390/atmos12060759.

Zhou, X., Xie, M., Zhao, M., Wang, Y., Luo, J., Lu, S., Li, J., Liu, Q., 2023. Pollution characteristics and human health risks of $PM_{2.5}$-bound heavy metals: a 3-year observation in Suzhou, China. Environ. Geochem. Health, 45, 5145-5162. https://doi.org/10.1007/s10653-023-01568-x.

Zhu, B.Q., Chen, Y.W., Peng, J.H., 2001. Lead isotope geochemistry of the urban environment in the Pearl River Delta. Appl. Geochem., 16, 409-417. https://doi.org/10.1016/S0883-2927(00)00047-0.

Zhuang, X.G., Querol, X. Zeng, R.S., Xu, W.D., Alastuey, A., Lopez-Soler, A., Plana, F., 2000. Mineralogy and geochemistry of coal from the Liupanshui mining district, Guizhou, South China. Int. J. Coal Geol., 45, 21-37. https://doi.org/10.1016/S0166-5162(00)00019-7.

Tables

Table 1. Variations (Mean, Min and Max) of PM2.5-bound MM concentrations (ng m^{-3}) during the sampling period (November 2019 to December 2020). Mean and standard deviation (σ) include all samples of this study (n = 57).

	Ag	**Al**	**As**	**Cd**	**Co**	**Cr**	**Cu**	**Fe**	**Hg**	**Mn**	**Ni**	**Sb**	**Sn**	**Pb**	**Ti**	**U**	**V**	**Zn**
Mean	0.285	349	3.97	1.82	0.153	3.31	56.8	295	0.190	32.0	1.34	4.81	3.38	65.7	26.3	0.039	1.20	444
σ	0.467	271	2.80	1.43	0.090	5.31	90.9	198	0.134	43.9	1.31	3.83	2.31	71.6	19.2	0.031	0.700	545
Min	0.012	15.4	0.674	0.179	0.028	0.412	2.28	70.9	0.010	2.83	0.018	0.646	0.784	3.29	4.29	0.001	0.137	22.5
Max	3.47	1427	11.2	5.95	0.477	40.5	641	1033	0.576	275	7.01	16.9	10.8	392	98.2	0.142	3.95	2054

1022 **Table 2.** Pb isotopic compositions in estimated natural soil, urban aerosol and relics from China and

1023 southeast Asian.

			$^{207}Pb/^{206}Pb$	$^{208}Pb/^{206}Pb$
Estimated natural soil (Bing-Quan et al., 2002)				
Northeast China	min		0.8673	2.1084
Northeast China	max		0.8511	2.0800
North China	min		0.9615	2.2817
North China	max		0.8621	2.1457
Indochina	min		0.8410	2.0698
Indochina	max		0.8278	2.0613
Aerosol from urban cities (Bollhöfer and Rosman, 2000)				
Vietnam	Heni		0.8569	2.1020
Vietnam	Huzhimin		0.8658	2.1039
Thailand	Bangkok		0.8873	2.1331
Malaysia	Kuala Lummpur		0.8764	2.1122
Indonesia	Bandung		0.9116	2.1568
Neolitic relics from southeast Asia (Pryce et al., 2014)				
Thailand	Khao SaKaeo	400-200 BC	0.7695	2.0063
Thailand	Non Pa Wai	1000-300 BC	0.7785	1.8921
Thailand	Phu Lon	1000 BC	0.7877	1.9534
Vietnam	Lang Nhon	NA	0.7958	2.0531

1024 NA: not available

1025

1026

1027 **Table 3.** Estimation of human health risk from PM2.5 inhalation in Hanoi: detailed indices (HQ_i and

1028 CR_i) per element and cumulative indices (HI, TCR).

	HQ_i	CR_i
Ag	NA	NA
Al	$7.4\ 10^{-5}$	NA
As	$2.9\ 10^{-4}$	$6.3\ 10^{-6}$
Cd	$2.1\ 10^{-4}$	$3.0\ 10^{-6}$
Co	$2.7\ 10^{-5}$	$5.0\ 10^{-7}$
Cr	**$3.1\ 10^{-2}$**	**$8.8\ 10^{-5}$**
Cu	$1.5\ 10^{-3}$	NA
Fe	NA	NA
Hg	$6.7\ 10^{-6}$	NA
Mn	$6.6\ 10^{-4}$	NA
Ni	$9.5\ 10^{-5}$	$1.2\ 10^{-7}$
Pb	**$2.2\ 10^{-2}$**	$3.2\ 10^{-7}$
Sb	**$1.8\ 10^{-2}$**	NA
Sn	NA	NA
Ti	$2.8\ 10^{-4}$	NA
U	$1.1\ 10^{-6}$	NA
V	$1.8\ 10^{-4}$	$3.7\ 10^{-6}$
Zn	$1.7\ 10^{-3}$	NA

	HI	*TCR*
Total	$7.6\ 10^{-2}$	$1.0\ 10^{-4}$

1029 NA: not available

1030

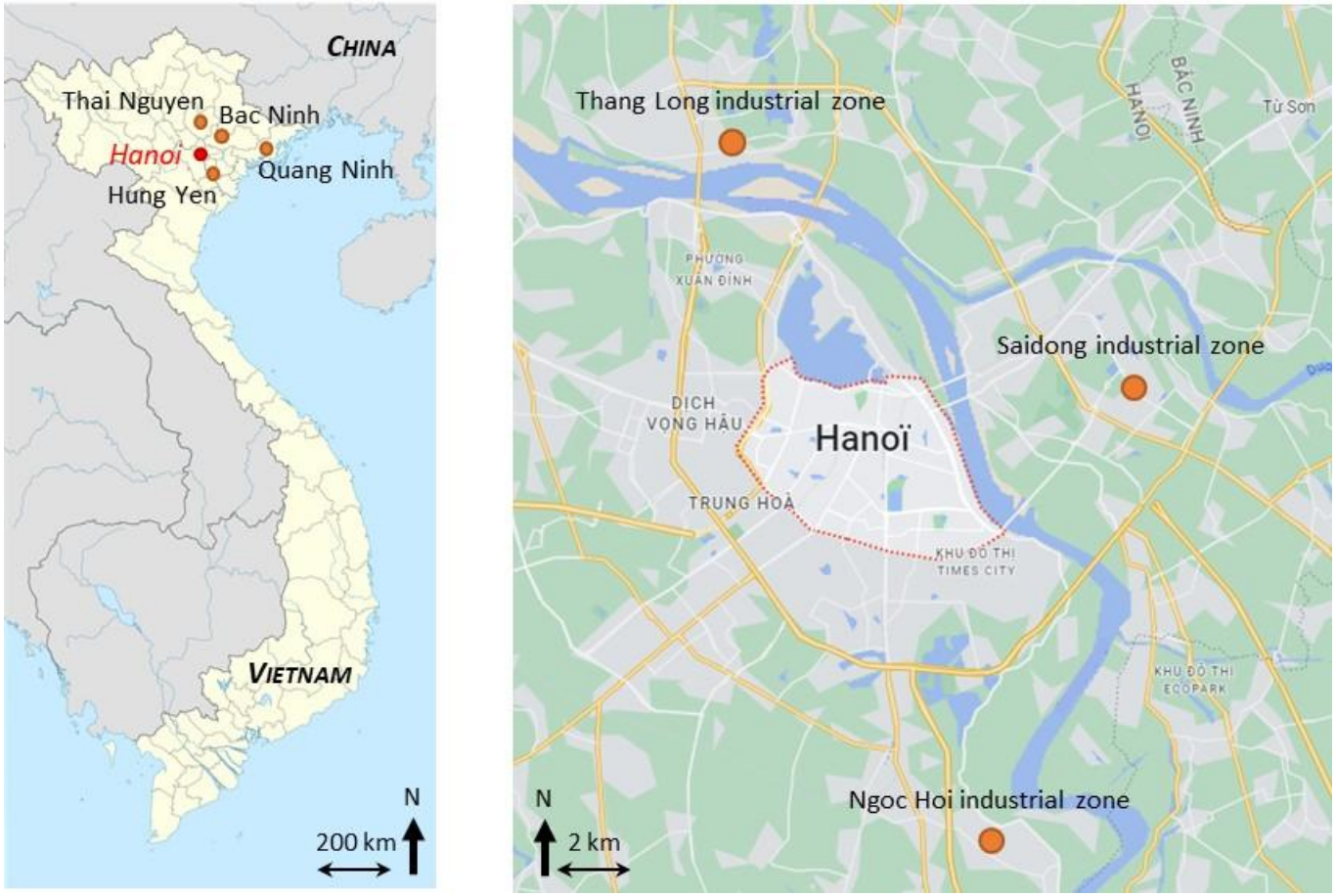

Figure 1: Localisation of sampling site

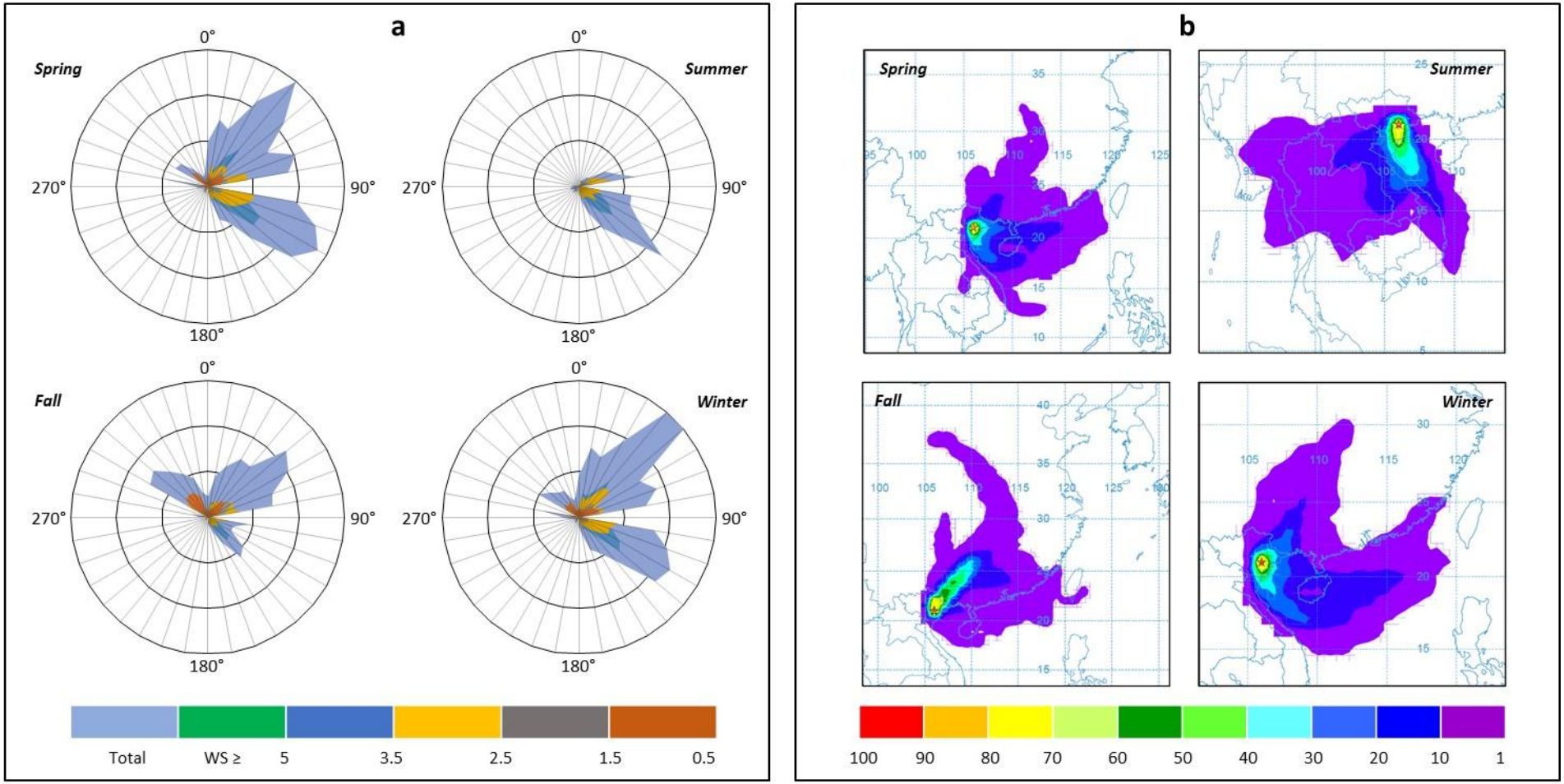

Figure 2: Wind roses (a) and trajectory frequencies (b) grouped by seasonal variations during the sampling period. Colour scales of wind speed (WS) and trajectory frequencies are expressed in m s-1 and %, respectively (NOAA HYSPLIT model, https://www.ready.noaa.gov/HYSPLIT.php).

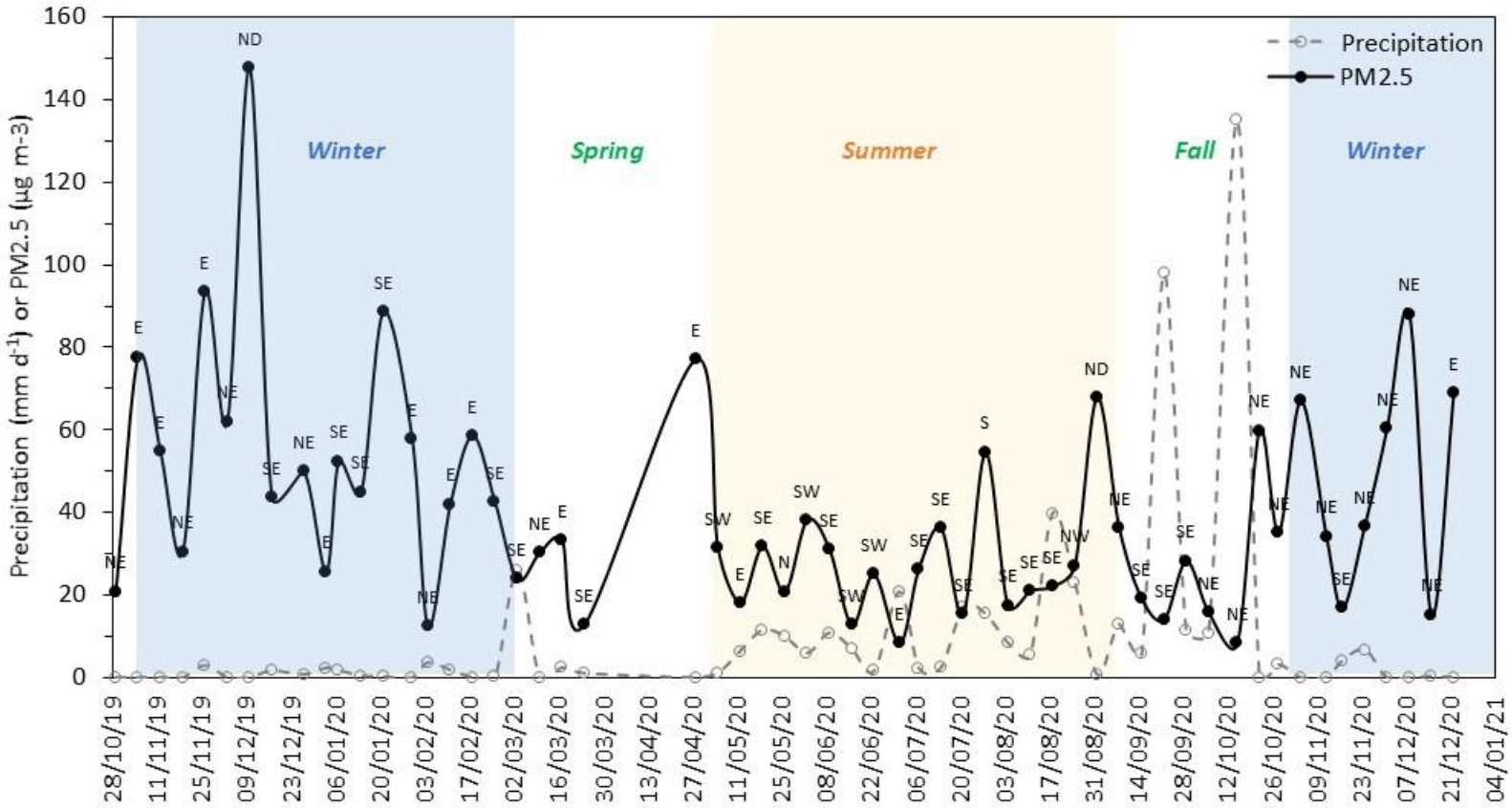

1037

1038 **Figure 3**: Seasonal variations in PM2.5 concentrations (µg m^{-3}) and precipitation (mm d^{-1}). Abbreviations indicate the wind direction: Northeast (NE), East (E),

1039 Southeast (SE), Southwest (SW), Northwest (NW) and not defined (ND)

1040

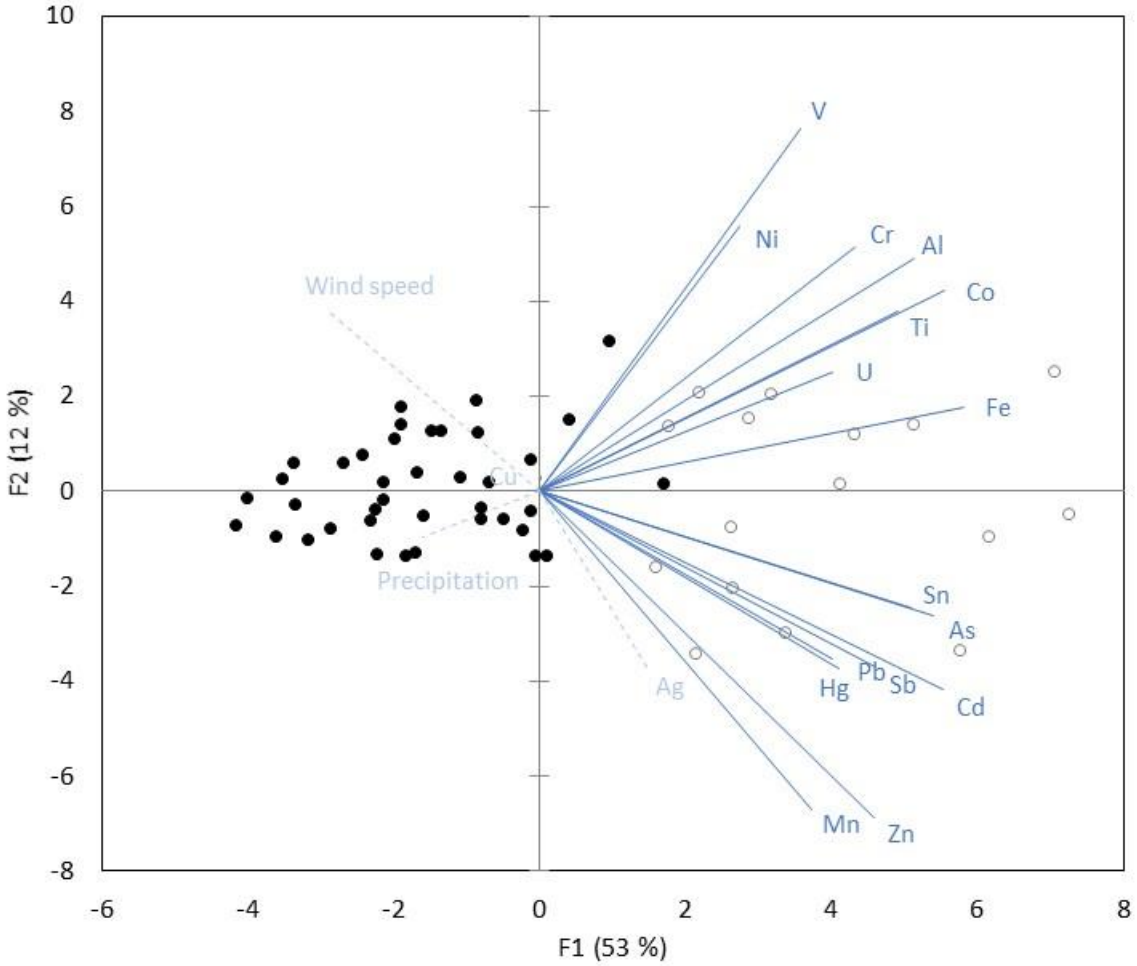

Figure 4: Statistical analyses (PCA-HCA) of MM concentrations in PM2.5 during the sampling period (November 2019 to December 2020). The contribution of the active and illustrative variables on axes F1 and F2 are presented in solid and dotted lines, respectively. The distribution of samples in clusters C1 and C2 are presented in solid and open circles, respectively.

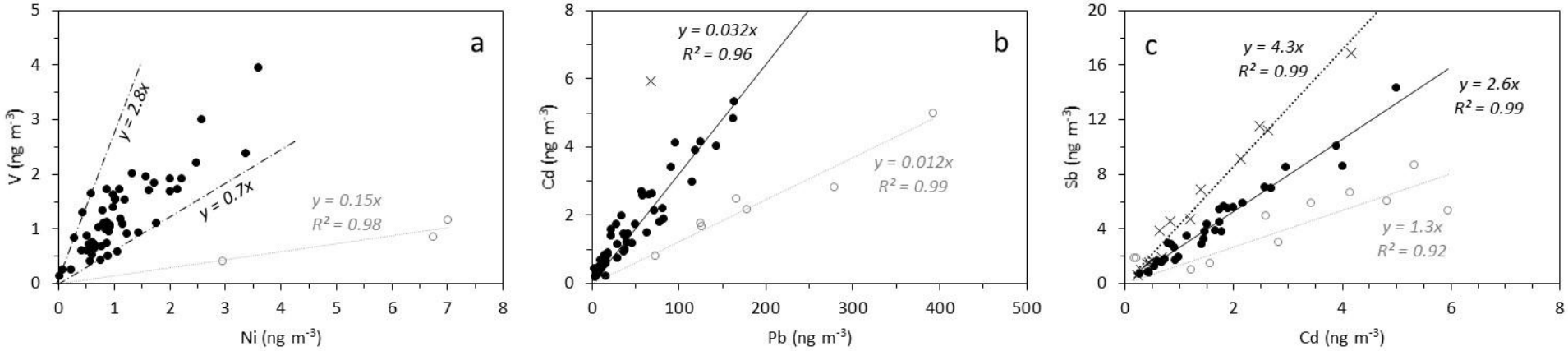

1045

1046 **Figure 5**: Elementary ratios in PM2.5 collected during the sampling period (November 2019 to December 2020): a) V/Ni, b) Cd/Pb, c) Sb/Cd and d) Al/Ti

1047

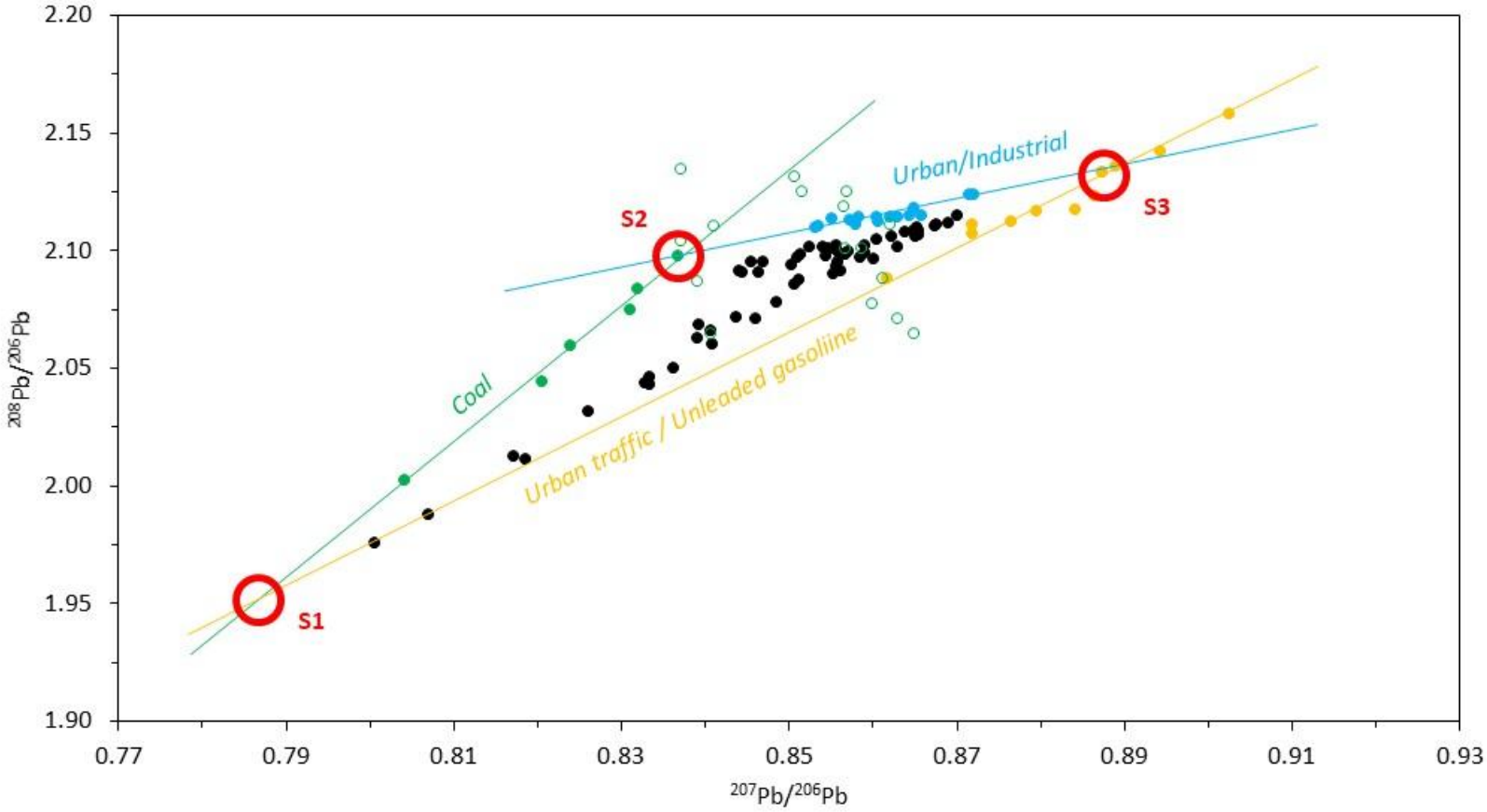

1048

1049 **Figure 6**: Pb isotopic ratios ($^{208}Pb/^{206}Pb$ *vs* $^{207}Pb/^{206}Pb$) in PM2.5 collected in Hanoi during the sampling period (in black). The coloured data comes from the

1050 literature, in green for Chinese coal mines (solid circles come from southern provinces), in blue for Chinese urban and industrial activities and in

1051 orange for petroleum-related activities (*e.g.,* from road traffic in Asian megacities, unleaded Chinese gasoline and Russian oil fields).

1052

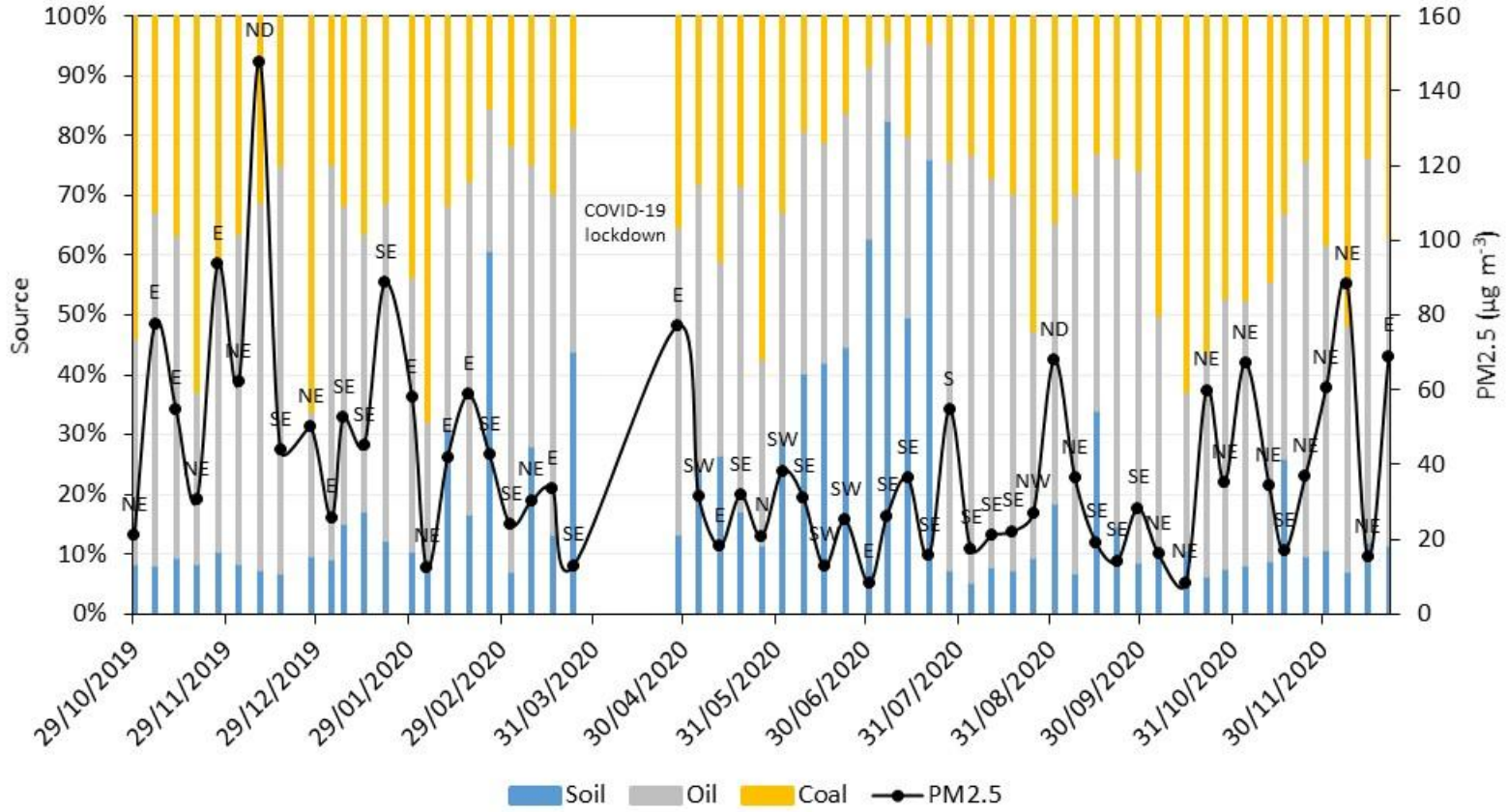

1053

1054 **Figure 7**: Contribution of Pb sources from 'natural' soil, 'oil' and coal to PM2.5 during the sampling period (November 2019 to December 2020).

1055 Abbreviations indicate the wind direction: Northeast (NE), East (E), Southeast (SE), Southwest (SW), Northwest (NW) and not defined (ND)

1056